HETEROCYCLES, Vol. 75, No. 10, 2008, pp. 2381 - 2413. © The Japan Institute of Heterocyclic Chemistry
Received, 25th January, 2008, Accepted, 21st March, 2008, Published online, 28th March, 2008. REV-08-631

CHEMISTRY AND APPLICATIONS OF 4,5-DIAZAFLUORENES

Katsuhiko Ono* and Katsuhiro Saito

Department of Materials Science and Engineering, Nagoya Institute of Technology, Gokiso, Showa-ku, Nagoya 466-8555, Japan; e-mail: ono.katsuhiko@nitech.ac.jp

Abstract – The synthesis, molecular structures, reactions, and properties of 4,5-diazafluorene derivatives have been studied because of their potential applications in organic devices. These compounds have similarities to 2,2′-bipyridyl and 1,10-phenanthroline derivatives. They also exhibit unique reactivities and properties different from these compounds due to the fluorene moieties. The applications of 4,5-diazafluorenes have been widely investigated in various research fields to afford new functional materials such as electron-transporting materials, organic emitters, emissive complexes, sensing elements, solar sensitizers, and antibiotics. This article describes the chemistry and applications of 4,5-diazafluorenes.

INTRODUCTION

9*H*-Cyclopenta[2,1-*b*:3,4-*b*′]dipyridine (4,5-diazafluorene) derivatives have attracted considerable attention for their molecular structures, reactions, and unique properties because of their potential applications in organic devices. These compounds have similarities to 2,2′-bipyridyl and 1,10-phenanthroline derivatives. They have high electron affinities and react with nucleophilic reagents at the 3,6-positions, *e.g.*, direct arylation and alkylation. Furthremore, these compounds can form various complexes by coordination to metals such as Fe, Cu, Ag, Eu, and Ru. On the other hand, 4,5-diazafluorenes reveal unique reactions and properties that are different from those of 2,2′-bipyridyl and 1,10-phenanthroline due to the fluorene moieties. 4,5-Diazafluorene possesses a reactive methylene unit at the 9-position, thereby affording various kinds of derivatives. The fluorene skeletons also affect the chelation of the compounds to the metals, *e.g.*, bond angles and bond lengths. Since 4,5-diazafluorene derivatives have potential applications as well as 2,2′-bipyridyl and 1,10-phenanthroline derivatives, their properties have been widely investigated in various research fields. In this paper, we discuss the chemistry and applications of 4,5-diazafluorene.

1. SYNTHESIS OF 4,5-DIAZAFLUORENES

4,5-Diazafluorene (**1**) has been synthesized *via* 4,5-diazafluoren-9-one (**6**), as shown in Scheme 1. The synthesis of compound (**6**) was studied in detail by Plater *et al.*[1] They prepared compound (**6**) by the one-step oxidative ring contraction of phenanthroline (**2**) using a previously reported method.[2] However, the yield was approximately 20%. Under the given reaction conditions, 2,2′-bipyridyl-3,3′-dicarboxylic acid was obtained as a by-product. Therefore, they considered that the by-product was formed *via* the oxidation of compound (**3**). The desired reaction pathway requires a rapid benzil-benzilic acid ring contraction (**3** → **4**). By increasing the alkali concentration and adding a dilute solution of $KMnO_4$ slowly, the preferred ring contraction proceeded. Thus, the yield of **6** increased to 55–60% and the compound was obtained in the form of yellow crystals (mp = 218–219 °C). Starting from 20 g of commercial phenanthroline (**2**), 10–12 g of **6** can be obtained. Compound (**1**) was synthesized by the Wolff-Kishner reaction of **6** with hydrazine monohydrate in a Teflon-lined bomb at 180 °C for 6 h. The product was obtained as colorless crystals (mp = 170–171 °C) with a yield of 75%.

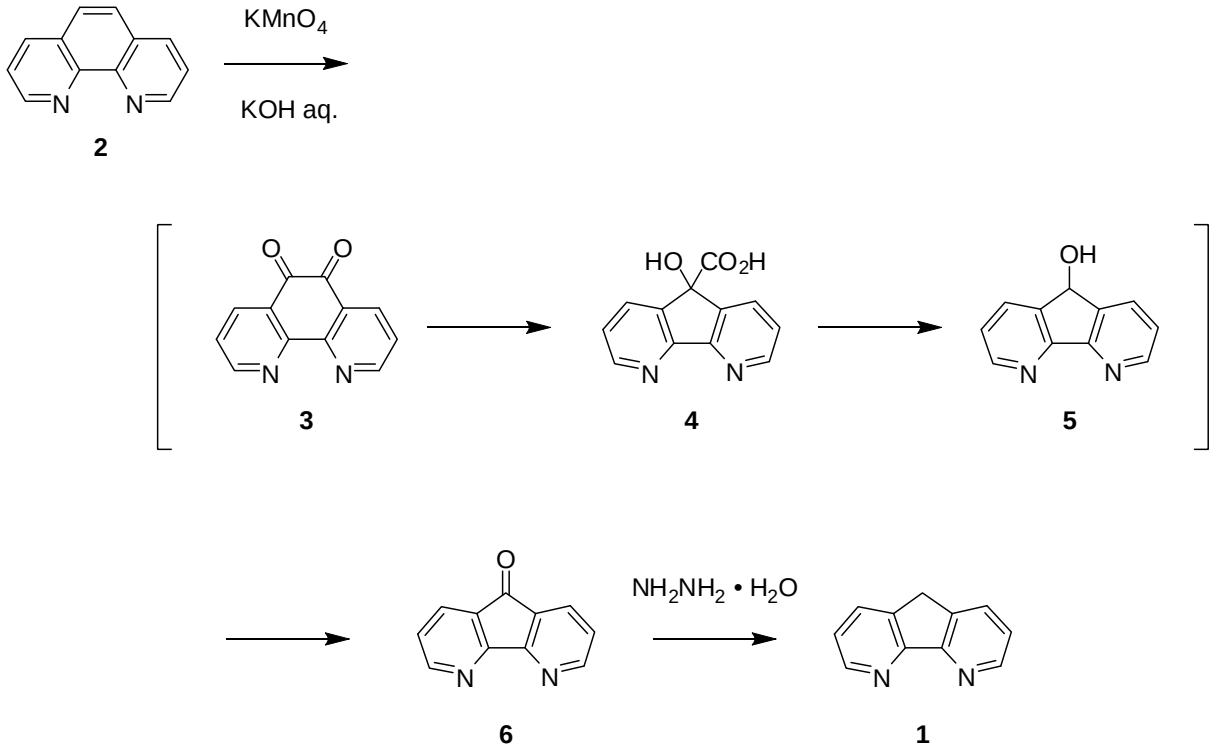

Scheme 1. Synthesis of 4,5-diazafluorene (**1**).

3,3′-Methylene-2,2′-biquinoline (**9a**) was synthesized by Thummel *et al.*,[3] as shown in Scheme 2. This compound is one of the benzo derivatives comprising a 4,5-diazafluorene skeleton. Compound (**9a**) was synthesized with a yield of 47% by the condensation reaction of 2-aminobenzaldehyde (**7a**) with 1,2-cyclopentanedione (**8**) in the presence of KOH. The compound was obtained as a yellow solid (mp

= 281–283 °C). Its properties were compared to those of 3,3′-dimethylene-, trimethylene-, and tetramethylene-2,2′-biquinolines (n: 2−4) with regard to the dihedral angles of 2,2′-biquinolines and their π-conjugations. The long absorption band of **9a** showed a well-resolved fine structure, which is attributed to the rigid, planar molecular structure. As the number of carbon atoms in the 3,3′-bridge was increased from two to four, the band was observed to shift to a higher energy with a decrease in the absorption intensity. This observation was explained by a decrease in the conjugative interaction between the two quinoline rings. Furthermore, dimethyl and diphenyl derivatives (**9b**) and (**9c**) were prepared by the condensation of **8** with 2-aminoacetophenone (**7b**) and 2-aminobenzophenone (**7c**), respectively.[4]

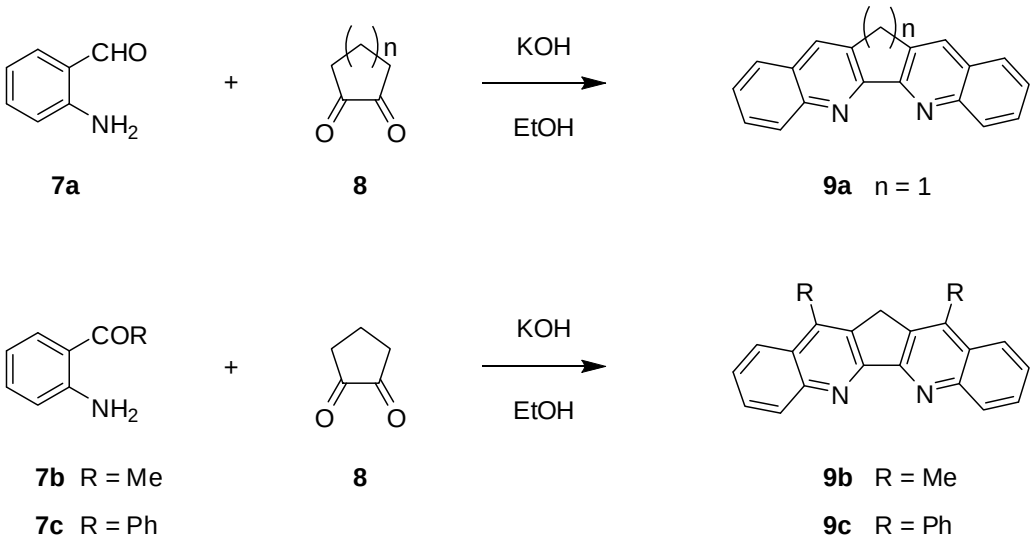

Scheme 2. Synthesis of 3,3′-methylene-2,2′-biquinolines (**9**).

2. MOLECULAR STRUCTURES OF 4,5-DIAZAFLUORENES

Connor *et al.*[5] reported the molecular structure of 4,5-diazafluorene (**1**) by X-ray crystallographic analysis (CCDC 110270) (Figure 1). Both the pyridine rings are planar (maximum deviation: 0.004(2) Å) and the dihedral angle between their best planes is 2.51(4)°; this value may be compared to that of the structure of fluorene in which the dihedral angle of the biphenyl moiety is 0.8(2)°. The bond lengths and angles are shown in Figure 1. Fun *et al.*[6] studied the molecular and crystal structures of 4,5-diazafluoren-9-one (**6**) by X-ray crystallographic analysis (Figure 2). The bond lengths and angles are similar to those of 4,5-diazafluorene (**1**). The molecule is planar as a whole and has a maximum deviation of 0.021(1) Å for the C9 atom. In the crystal, the molecules form two sets of parallel layers that are linked by C2–H···N5 intermolecular hydrogen bonds running parallel to the *b* axis.

(a)

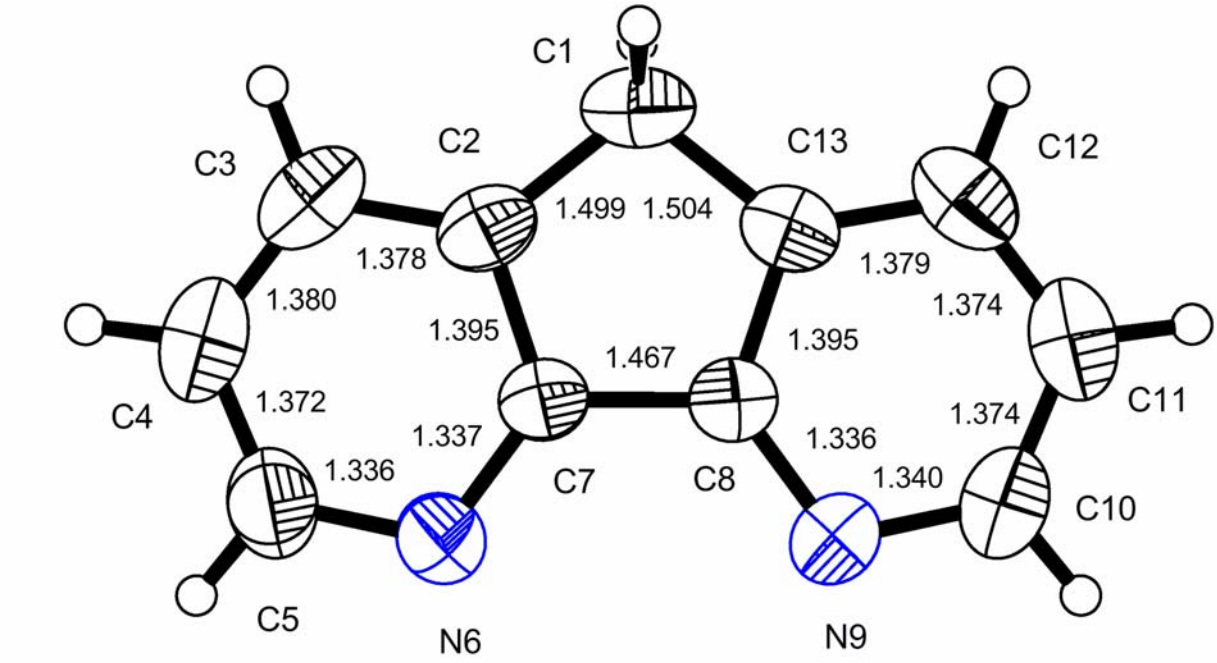

(b)

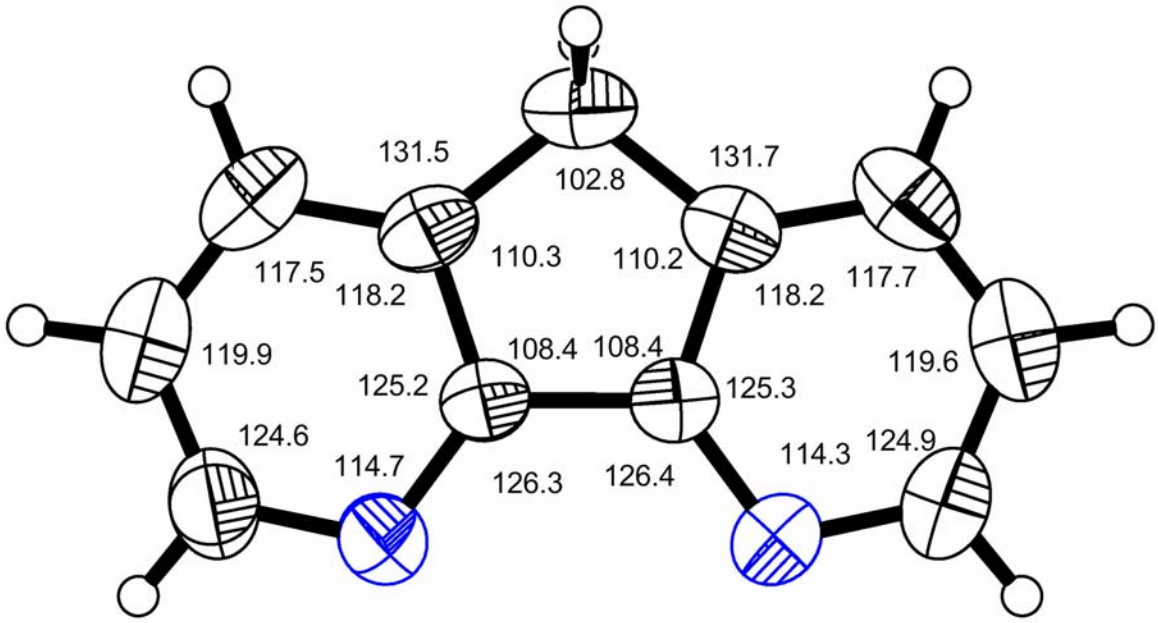

Figure 1. Bond lengths (Å) (a) and angles (°) (b) of 4,5-diazafluorene (**1**) (CCDC 110270).

(a)

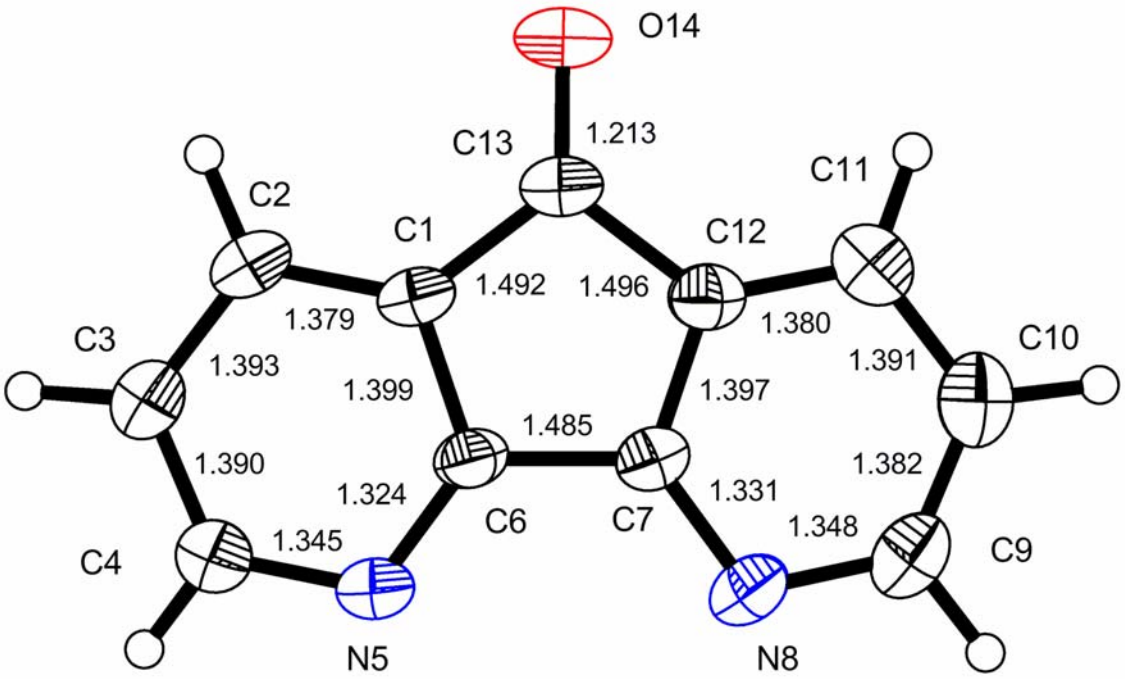

(b)

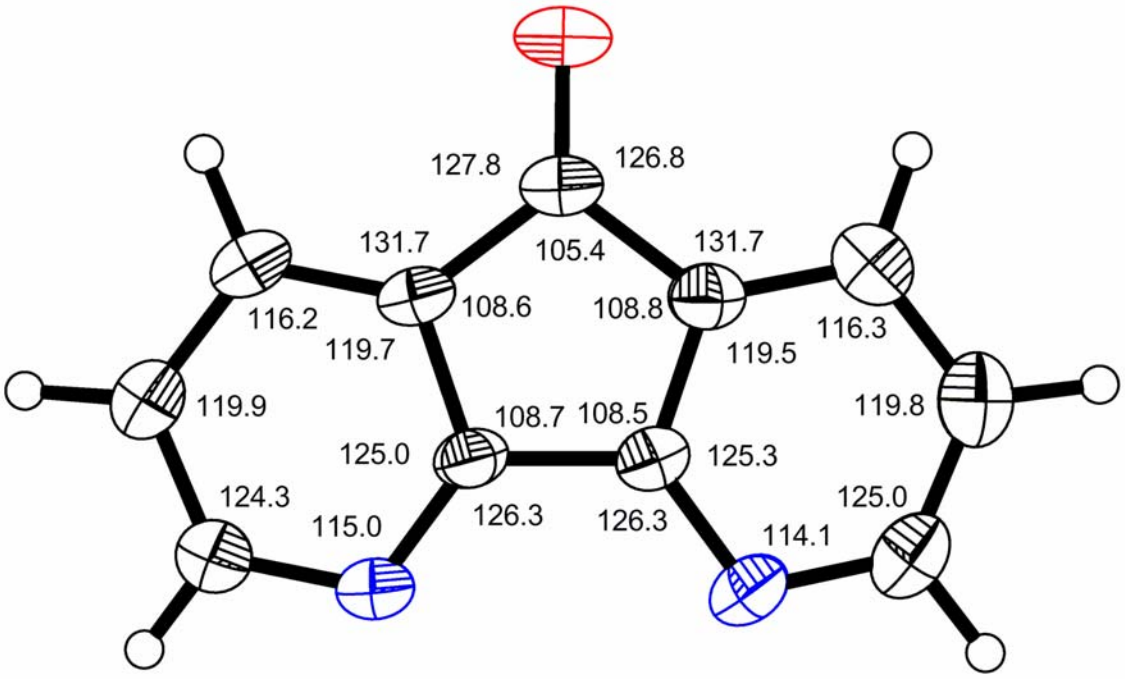

Figure 2. Bond lengths (Å) (a) and angles (°) (b) of 4,5-diazafluoren-9-one (**6**) (*Acta Cryst.*, 1995, **C51**, 2076).

3. REACTIONS OF 4,5-DIAZAFLUORENES

Several reactions that use 4,5-diazafluorene (**1**) and 4,5-diazafluoren-9-one (**6**) as starting reagents are described in this section.

A. Synthesis of 9,9′-bi-4,5-diaza-9*H*-fluorenylidene

The intramolecular energy-transfer and electron-transfer properties of supramolecular assemblies formed by dendritic complexes have attracted considerable attention. The 4,5-diazafluorene unit is useful as a

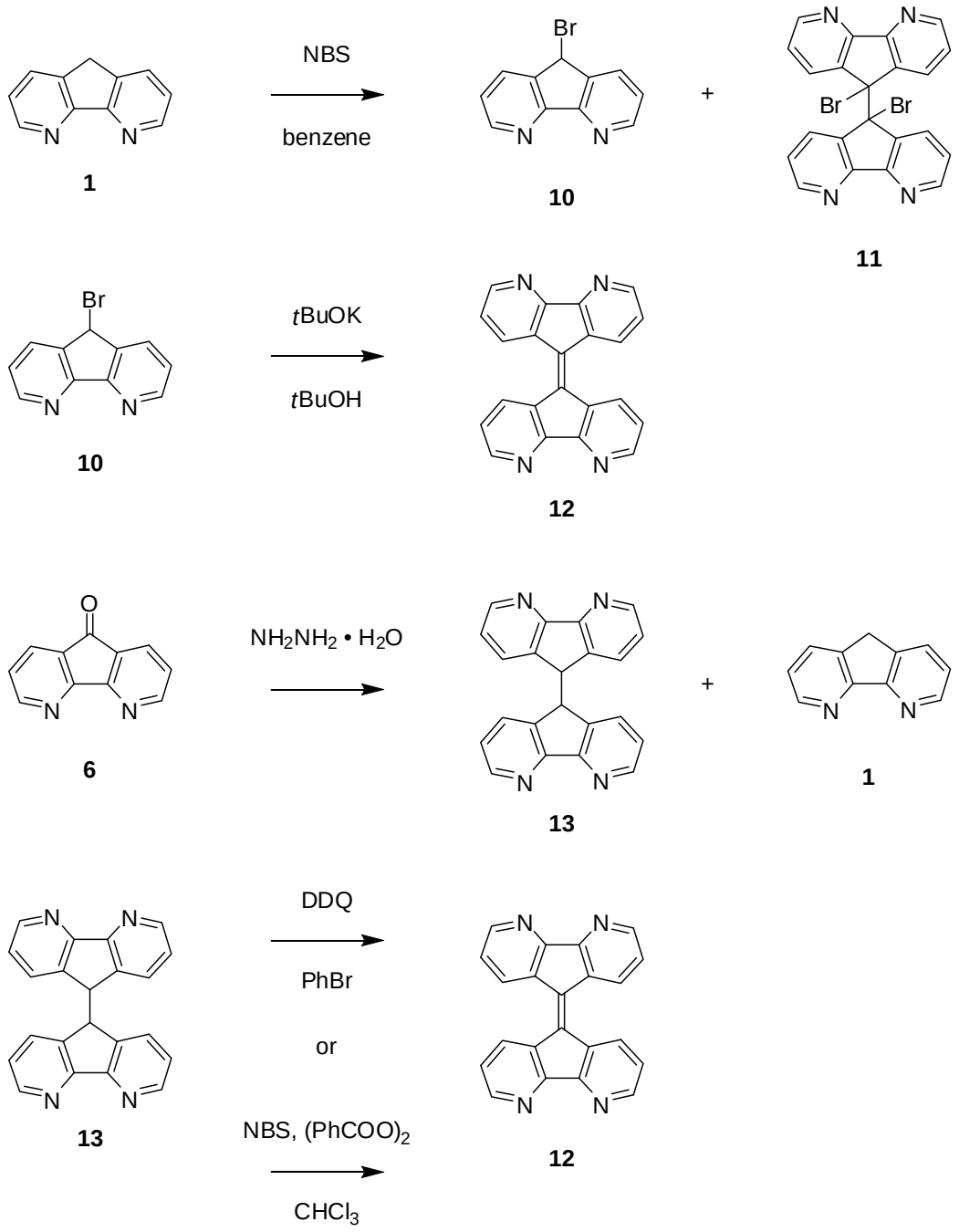

Scheme 3. Synthesis of 9,9′-bi-4,5-diaza-9*H*-fluorenylidene (**12**).

building component for the synthesis of bridging ligands. Connor *et al.*[5] studied the synthesis and properties of 9,9′-bi-4,5-diaza-9*H*-fluorenylidene (**12**) (Scheme 3). The bromination of 4,5-diazafluorene (**1**) using 1 equiv. of *N*-bromosuccinimide (NBS) in benzene yielded two products (**10**) and (**11**) with yields of 60% and 20%, respectively. The dehydrobromination of **10** with *t*BuOK in *t*BuOH afforded compound (**12**) with a yield of 90%. Another approach involved the dehydrogenation of **13** with 2,3-dichloro-5,6-dicyano-1,4-benzoquinone (DDQ) in bromobenzene. The oxidation was fast and led to a good yield (85%) of **12**. Compound (**13**) was obtained as the minor product (40% yield) in the Wolff-Kishner reduction of **6**.[7] Alternatively, the reaction of **13** with NBS in the presence of a catalytic quantity of dibenzoyl peroxide in chloroform also produced compound (**12**) in good yield (86%). Compound (**12**) was obtained in the form of an orange solid and did not melt below 320 °C. It is slightly soluble in benzene and readily soluble in polar solvents such as $CHCl_3$ and MeCN. The longest absorption maximum of **12** in chloroform was observed at 416 nm (log ε 4.31). The cyclic voltammetry of **12** in DMF solution indicated two quasi-reversible reductions at −0.67 and −1.13 V vs. saturated calomel electrode (SCE).

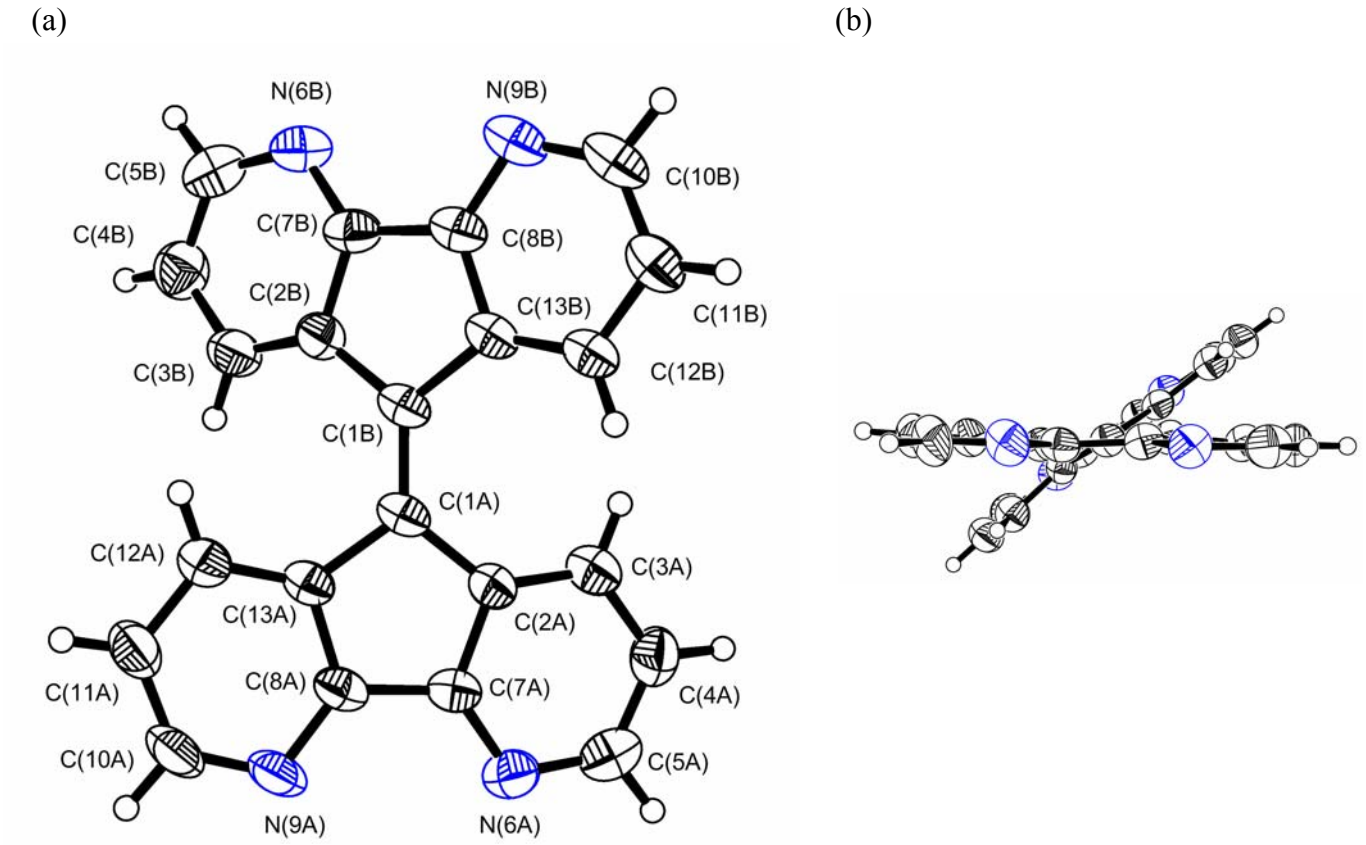

Figure 3. Molecular structure of 9,9′-bi-4,5-diaza-9*H*-fluorenylidene (**12**); (a) top view, (b) side view (CCDC 110269).

The molecular structure of 9,9′-bi-4,5-diaza-9*H*-fluorenylidene (**12**) was investigated by X-ray crystallographic analysis (CCDC 110269).[5] Figure 3 shows that the two diazafluorenylidene fragments are each nearly planar (maximum deviation: 0.1 Å), and the dihedral angle between these planes is 37.8°. The distance of the inter-ring double bond [C(1A)=C(1B)] is 1.385(4) Å. The mutual interference between the nonbonded H-atoms [C(3A)–H···H–C(12B) and C(12A)–H···H–C(3B)], which are separated by distances of 2.204(5) Å and 2.233(5) Å, respectively, is responsible for the observed distortion of the olefinic linkage. The molecular conformation is chiral, and both mirror-related conformations are present in the centrosymmetric crystal structure. The chiral conformation was caused by steric hindrance. Compound (**12**) formed a 1:1 charge-transfer complex with 7,7,8,8-tetracyanoquinodimethane (TCNQ), and the crystal structure was reported in a paper. Compound (**13**) was obtained in the form of colorless crystals. The longest absorption maximum was observed at 313 nm (log ε 4.76) in chloroform. The molecular structure of 9,9′-bi-4,5-diaza-9*H*-fluorenyl (**13**) is shown in Figure 4 (CCDC 110271).[5] The molecule adopts a gauche conformation around the bond linking the 4,5-diazafluorenyl moieties. The torsion angle around the aliphatic link is 67.39(6)° (H–C–C–H), and the length of the bond is 1.542(3) Å.

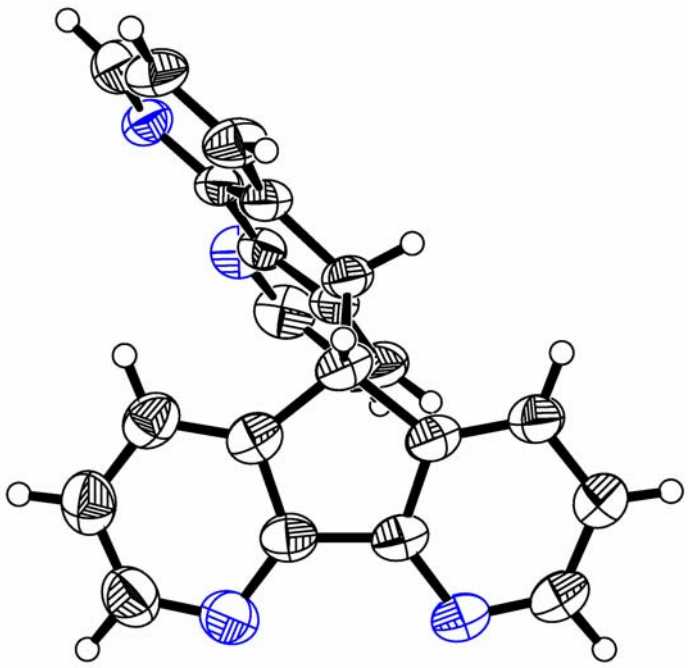

Figure 4. Molecular structure of 9,9′-bi-4,5-diaza-9*H*-fluorenyl (**13**) (CCDC 110271).

B. Reaction of 4,5-diazafluoren-9-one with trithiocarbonates

Sako *et al.*[8] reported the reaction of 4,5-diazafluoren-9-one (**6**) with trithiocarbonates (**14**) in the presence of triethyl phosphite [$P(OEt)_3$] (Scheme 4). The reactions afforded compounds (**15a**)–(**15d**) with yields of 43–55% in the form of yellow crystals. When one-third of the molar amount of ferrous sulfate ($FeSO_4$) was added to a solution of **15b**, the solution turned reddish yellow in color and orange precipitates were formed, indicating the presence of coordination with Fe^{2+} ions. Dai *et al.*[9] prepared the silver(I) and copper(I) complexes of **15a**–**15d** and investigated their properties and molecular assemblies. The molecular assembly of the silver complex $[Ag(\mathbf{15a})_2]ClO_4{\cdot}2CH_2Cl_2$ (CCDC 209123)[9a] is shown in Figure 5.

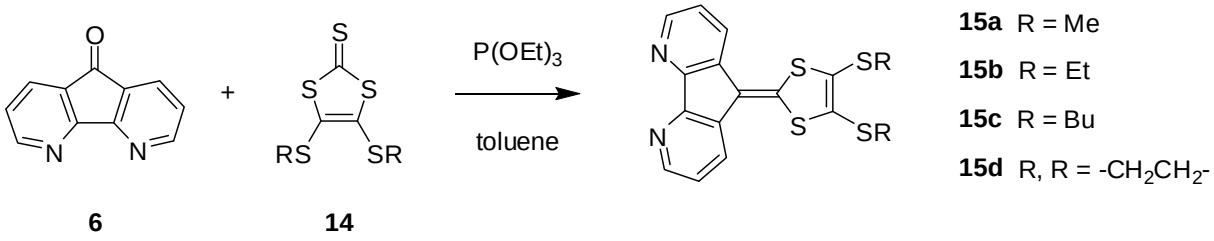

Scheme 4. Cross-coupling reactions of **6** with trithiocarbonates (**14**).

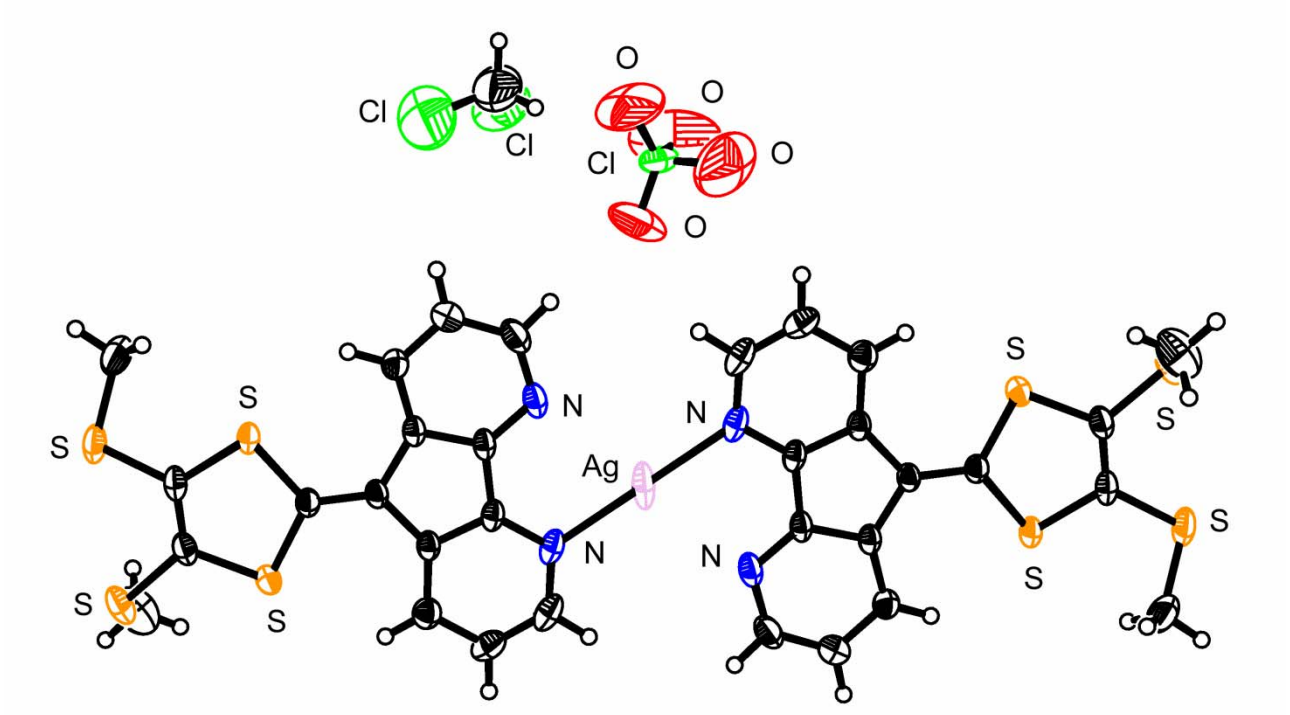

Figure 5. Crystal structure of $[Ag(\mathbf{15a})_2]ClO_4{\cdot}2CH_2Cl_2$ (CCDC 209123).

C. Reaction of 4,5-diazafluoren-9-one with amines and hydrazines

The reactions of 4,5-diazafluoren-9-one (**6**) with various amines and hydrazines were investigated. These products are used as the building blocks of functional polynuclear complexes. The condensation of **6** with aromatic amines was studied in detail by Rillema *et al.*[10] The reactions using aniline, 1,4-phenylenediamine, benzidine, and 4,4′-diaminodiphenylmethane in refluxing acetic acid afforded compounds (**16**)–(**19**) with yields of 40–73% (Scheme 5).

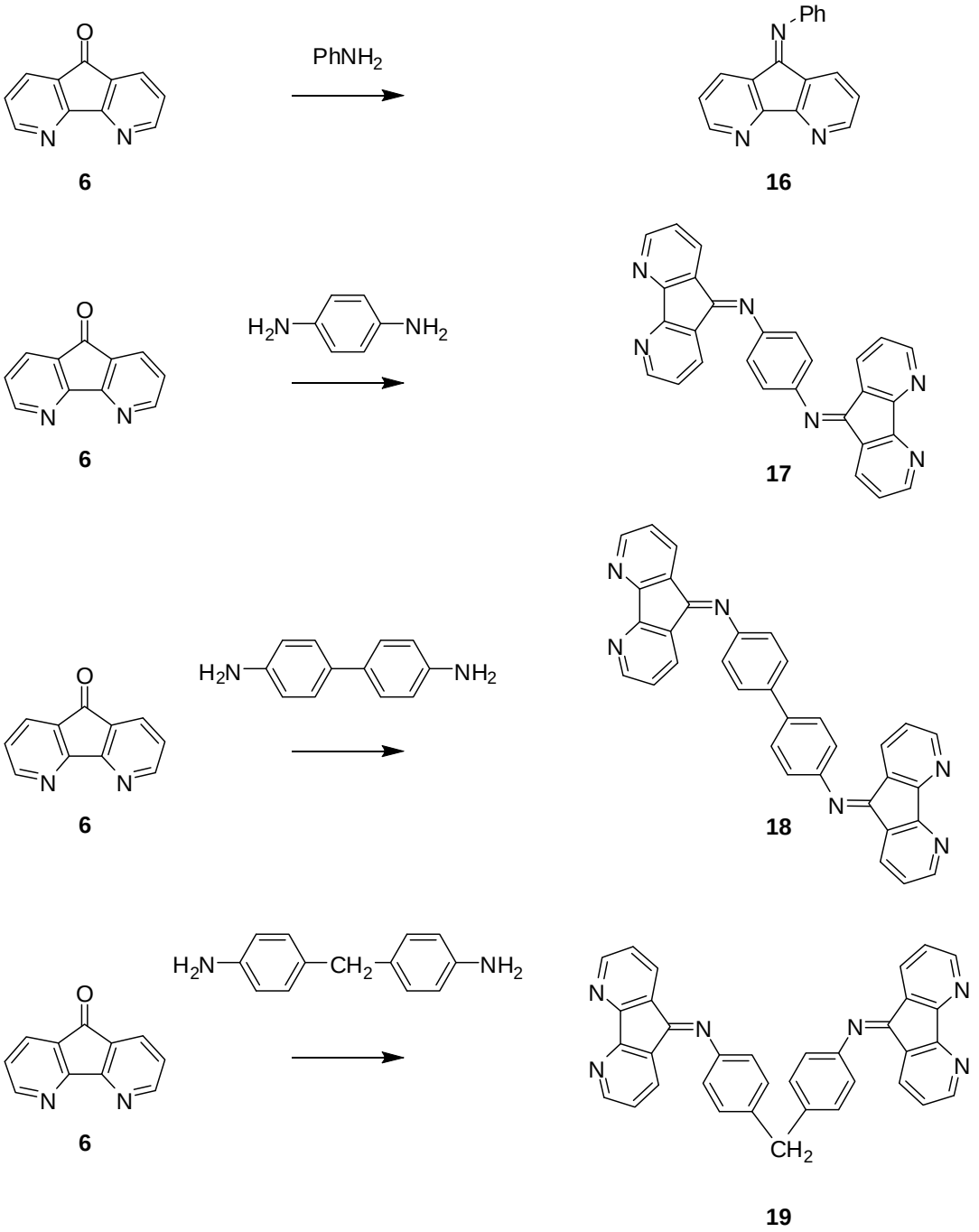

Scheme 5. Reactions of 4,5-diazafluoren-9-one (**6**) with amines.

The condensation of 4,5-diazafluoren-9-one (**6**) with hydrazine monohydrate was also studied by Rillema *et al.*,[10] and it was observed to yield hydrazones (**20**) and (**21**) (Scheme 6). The reactions involving phenylhydrazine and benzoylhydrazine afforded hydrazones (**22**) and (**23**), respectively.[11,12] Fun *et al.*[12] reported the molecular structure of **23** obtained by X-ray crystallographic analysis (Figure 6).

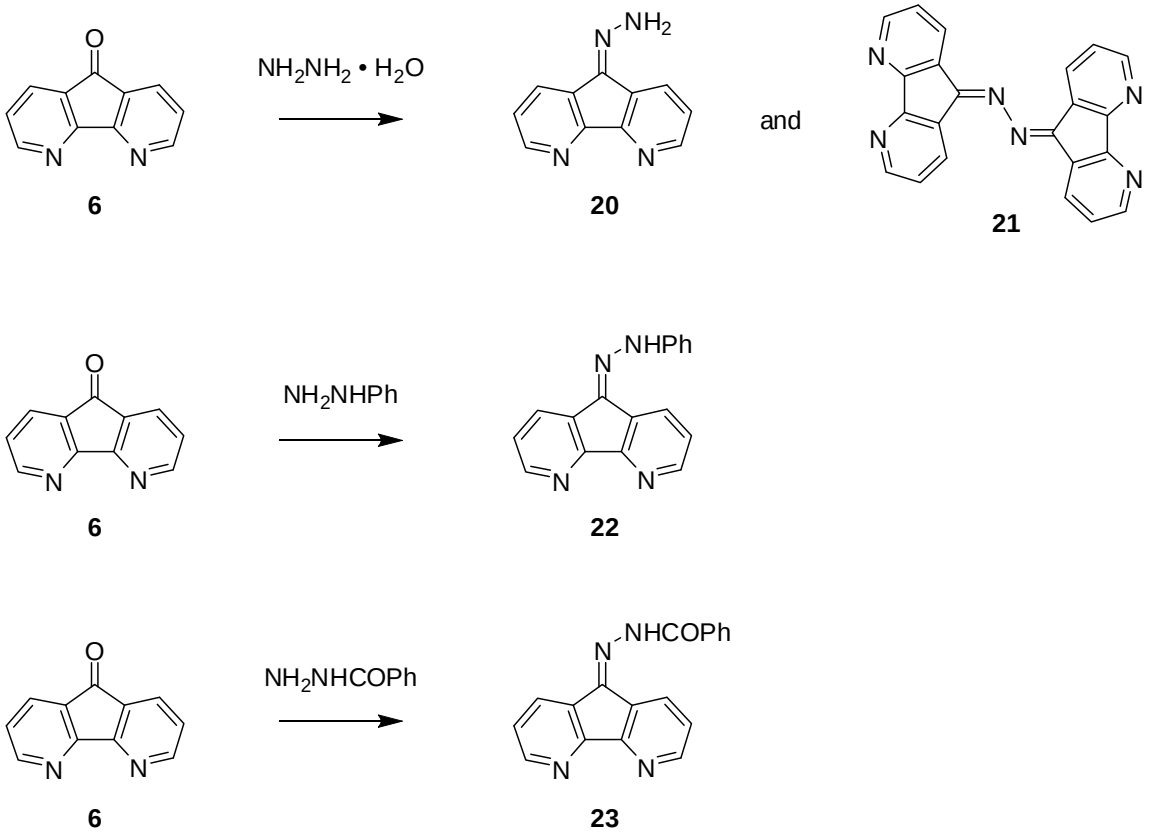

Scheme 6. Reactions of 4,5-diazafluoren-9-one (**6**) with hydrazines.

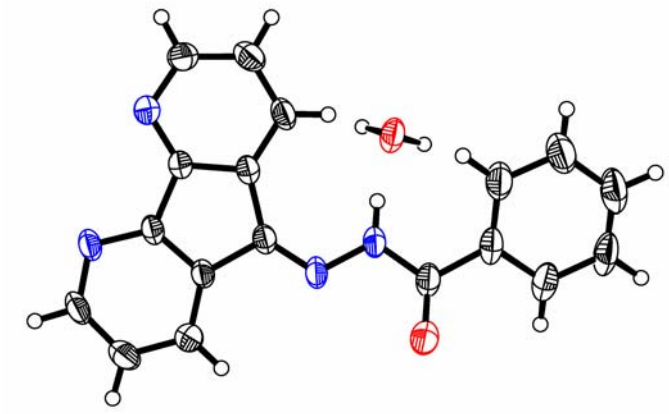

Figure 6. Molecular structure of **23** (*Acta Cryst.*, 2000, **C56**, 1017).

D. Synthesis and reactions of 9-diazo-4,5-diazafluorene

9-Diazo-4,5-diazafluorene (**25**) is a synthon for various functional materials, including 4,5-diazafluorene units. Two methods were reported for the synthesis of **25** (Scheme 7). Compound (**6**) reacted with tosylhydrazine to afford compound (**24**), which was treated with NaOH aq. to give compound (**25**) with a yield of 80%.[13] Compound (**25**) was prepared with a yield of 65% *via* the oxidation of compound (**20**) using HgO.[14] Compound (**25**) was used within a few days after its preparation because of its low stability.

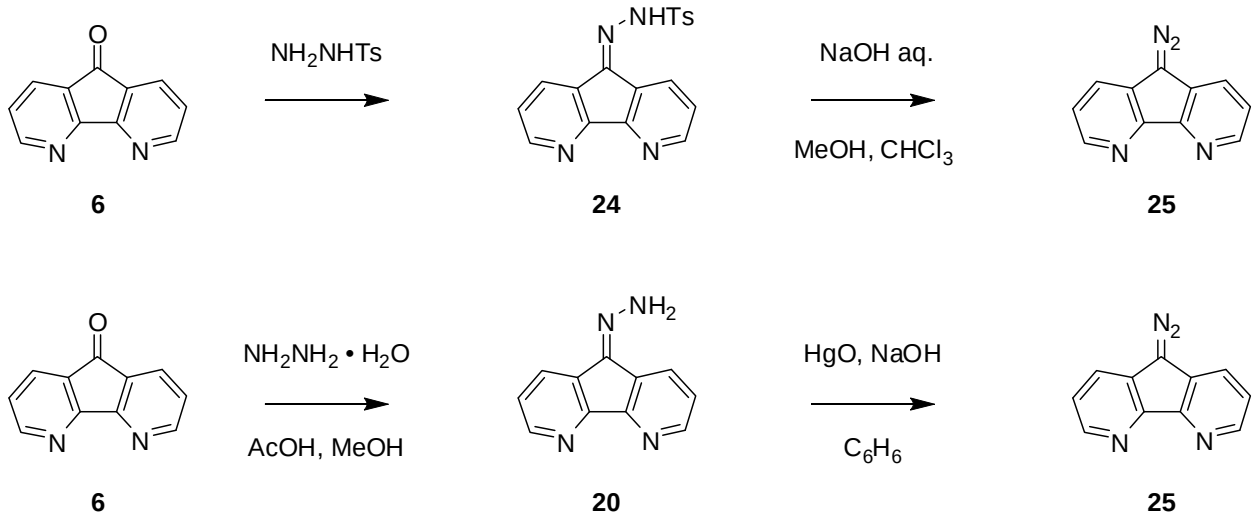

Scheme 7. Synthesis of 9-diazo-4,5-diazafluorene (**25**).

Compound (**25**) reacted with dithiones (**26**) and (**28**) in the presence of triphenylphosphine to provide compounds (**27**) and (**29**) with yields of 45% and 65%, respectively (Scheme 8).[13,15]

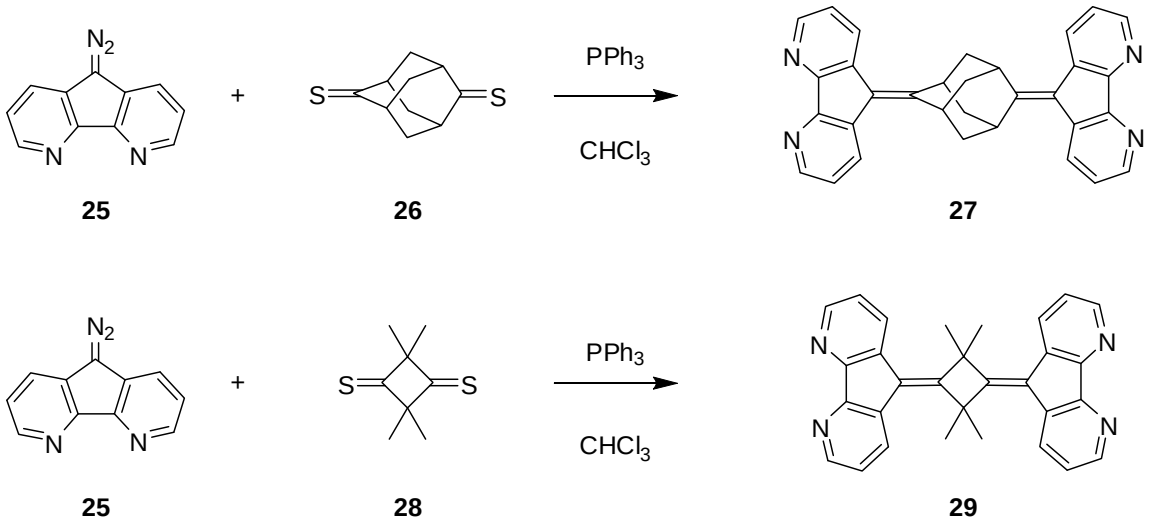

Scheme 8. Reactions of **25** with dithiones.

Warrener *et al.*[16] studied the 1,3-dipolar properties of 9-diaza-4,5-diazafluorene (**25**). Norbornadiene (**30**) reacted with **25** under high-pressure conditions (14 kbar, room temperature) to form a 1:1 adduct (**31**) (Scheme 9). The photolysis (λ = 300 nm) of pyrazoline yielded a cyclopropane ring (**32**). The reactions of **25** with olefins (**33**), (**35**), and (**37**) afforded compounds (**34**), (**36**), and (**38**) with yields of 40–98%.

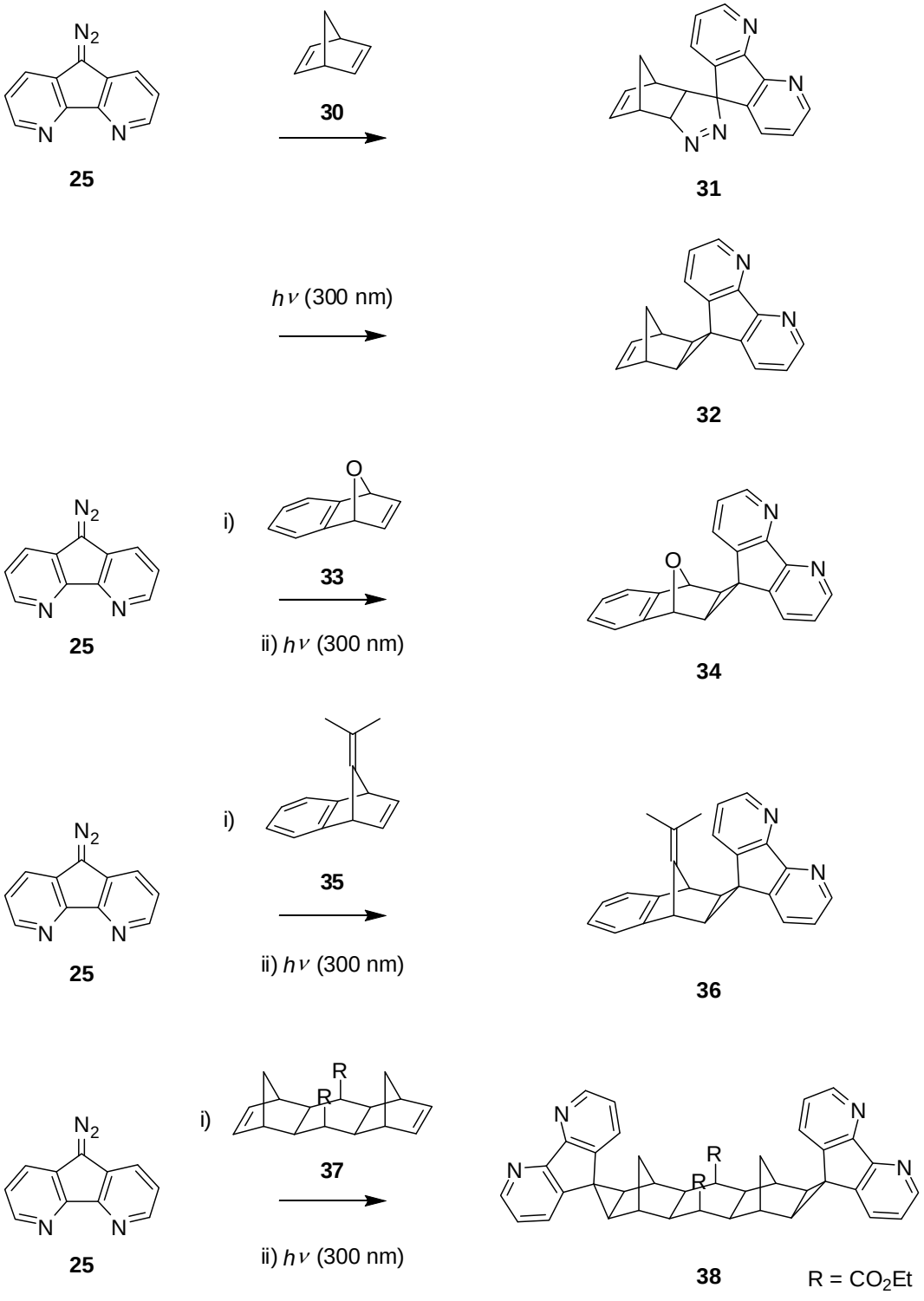

Scheme 9. Reactions of **25** with bicyclic olefins.

Compound (**25**) also reacted with cyclobutene (**39**) under high-pressure conditions to form a 1:1 adduct (**40**) (Scheme 10). The photolysis (λ = 300 nm) or thermolysis (in refluxing toluene) of the pyrazoline system yielded compound (**41**). The reaction of **25** with bis(cyclobutene) (**42**) afforded compound (**43**) with a yield of 63%. In these reactions, the bis(pyrazoline) system thermally decomposed to yield compound (**43**).

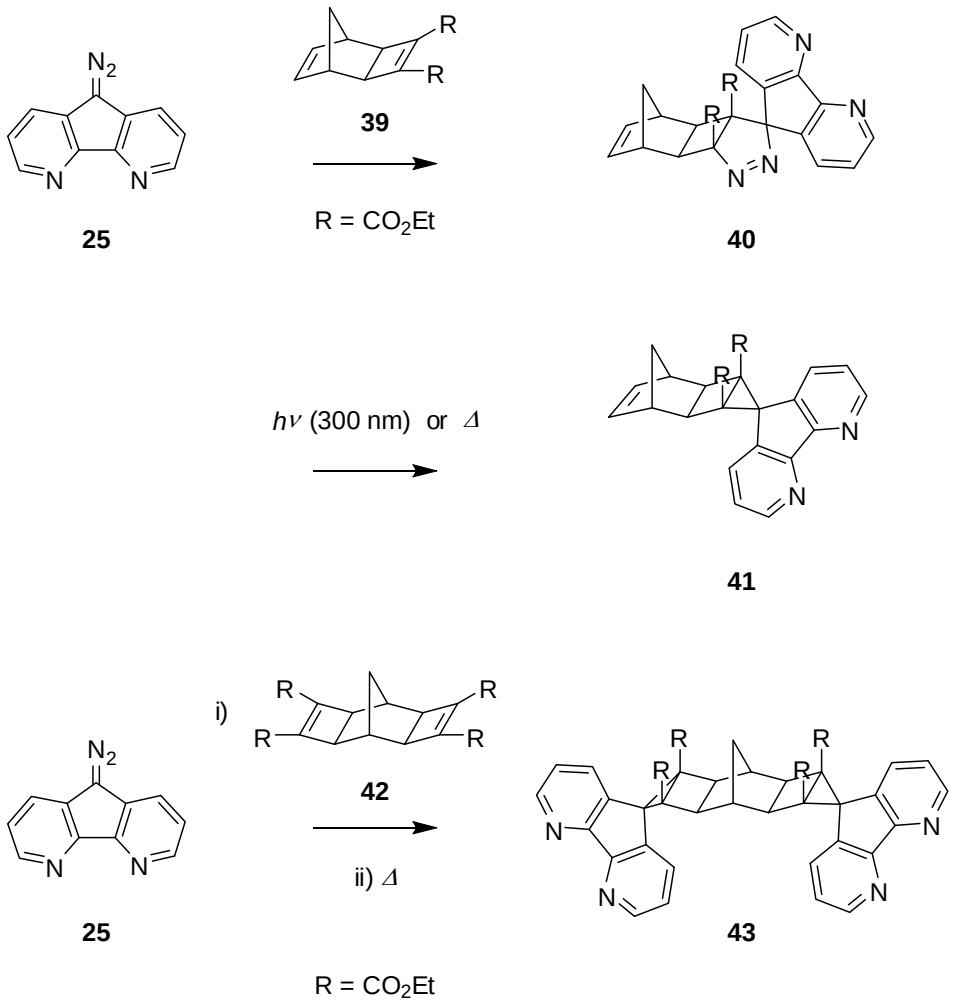

Scheme 10. Reactions of **25** with cyclobutenes.

E. Synthesis of 4,5-diazafluorene derivatives of Koelsch's radical

4,5-Diazafluorene derivatives of Koelsch's radical were prepared by Plater *et al.*[1] through the generation of heterocyclic free radicals. The synthesis of free radicals is shown in Scheme 11. The condensation of 4,5-diazafluorene (**1**) with benzaldehydes (**44**) in the presence of KOH afforded compounds (**45**) that reacted with **1** to yield compounds (**46**) as a mixture of tautomers. Compounds (**46**) were oxidized with $K_3Fe(CN)_6$ to provide Koelsch's radicals (**47**).

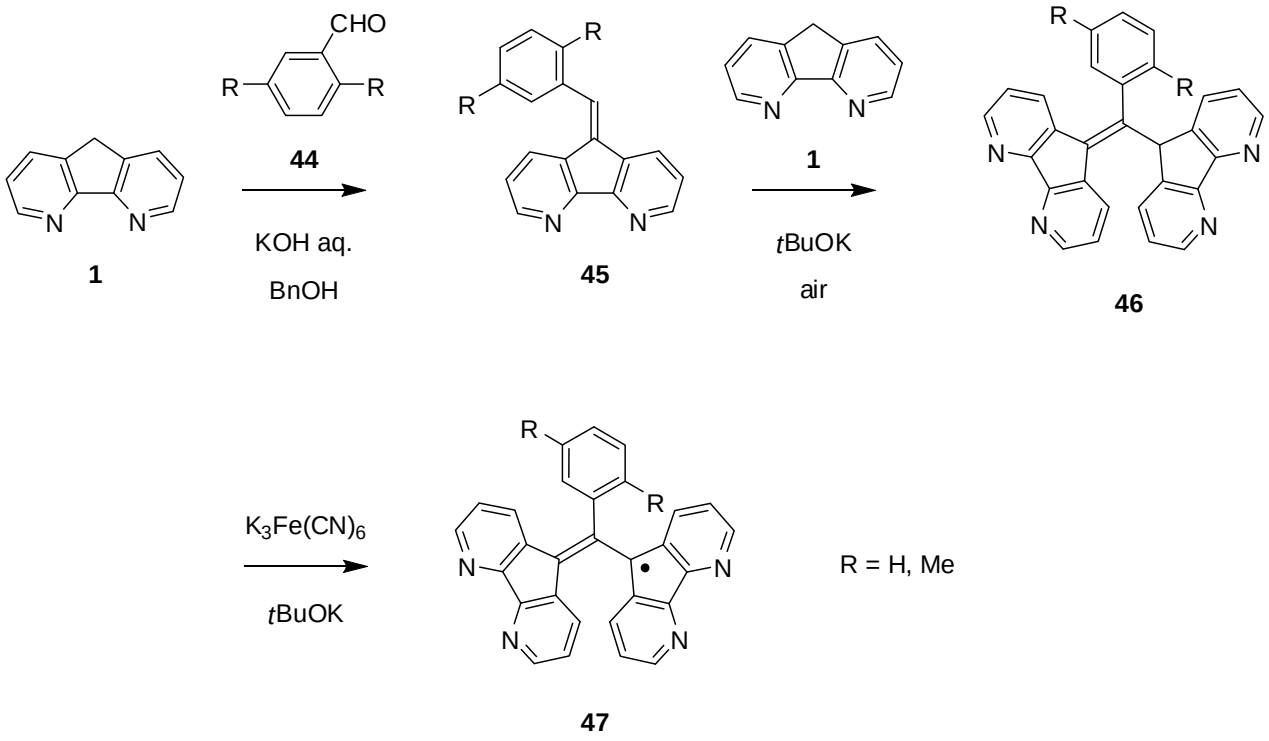

Scheme 11. Synthesis of heterocyclic free radicals (**47**).

F. Friedel-Crafts reactions of 4,5-diazafluoren-9-one with anisoles and phenol

We studied the Friedel-Crafts reactions of 4,5-diazafluoren-9-one (**6**) with anisole and phenol in the presence of sulfuric acid (Scheme 12).[17] The reactions of **6** with anisoles (**48**) afforded compounds (**49a**)–(**49c**) with yields of 70–90%. Compound (**51**) was also prepared with a yield of 52% by this reaction using phenol (**50**). These compounds were obtained in the form of colorless crystals (**49a**: mp = 275–276 °C, **49b**: mp = 208–209 °C, **49c**: mp = 211–212 °C, **51**: mp > 300 °C). Li *et al.*[18] reported that the Friedel-Crafts reaction of **6** with phenol (**50**) proceeded in the presence of hydrogen chloride to provide compound (**51**) with a yield of 40% (Scheme 13). Compound (**51**) reacted with an alkyl halide to afford compounds (**49a**) and (**52**), both with yields of 72%. For the preparation of **49a**, the synthetic method shown in Scheme 12 is useful. Since compound (**49a**) has a high electron affinity, it was investigated as an electron-transporting and hole-blocking material in the study of organic electroluminescent (EL) devices. Compounds (**49a**) and (**52**) were used as ligands for the application of europium(III) complexes, which have attracted considerable attention as red emitters. A ruthenium(II) complex containing **49a** as a polypyridyl ligand was synthesized and investigated as a dye sensitizer in the study of solar cells. These results are described in the next section.

The molecular structure and molecular packing of **49a** in the solid states were investigated by X-ray crystallographic analysis.[19] The molecule has a symmetrical structure about a twofold rotation axis

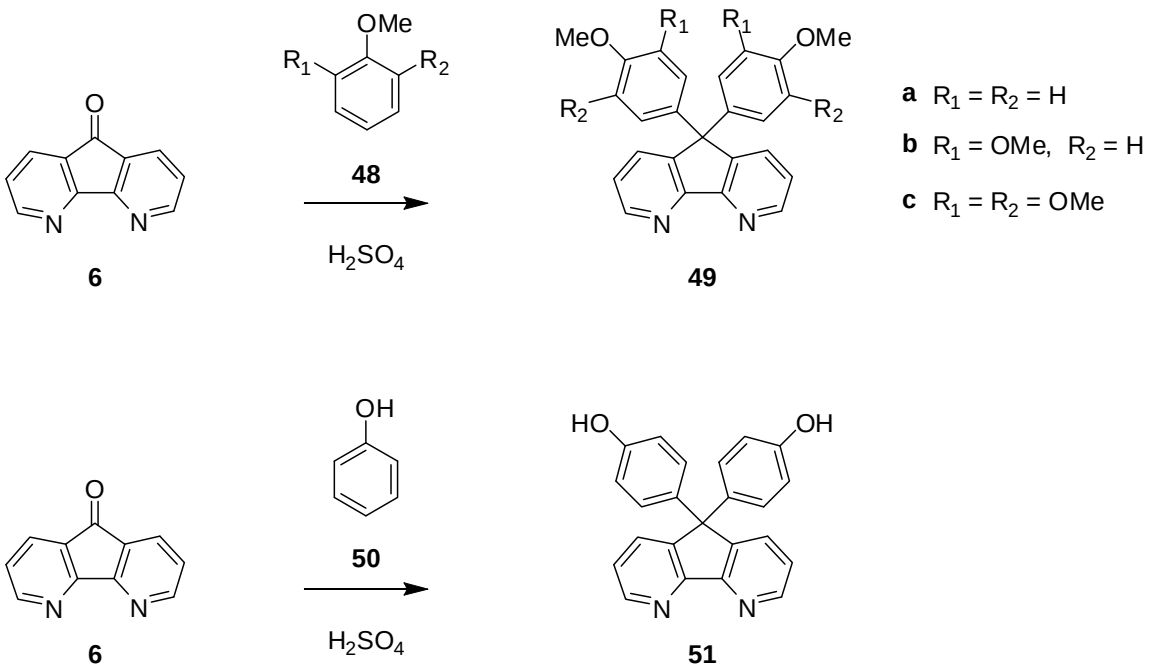

Scheme 12. Friedel-Crafts reactions of **6** in the presence of H_2SO_4.

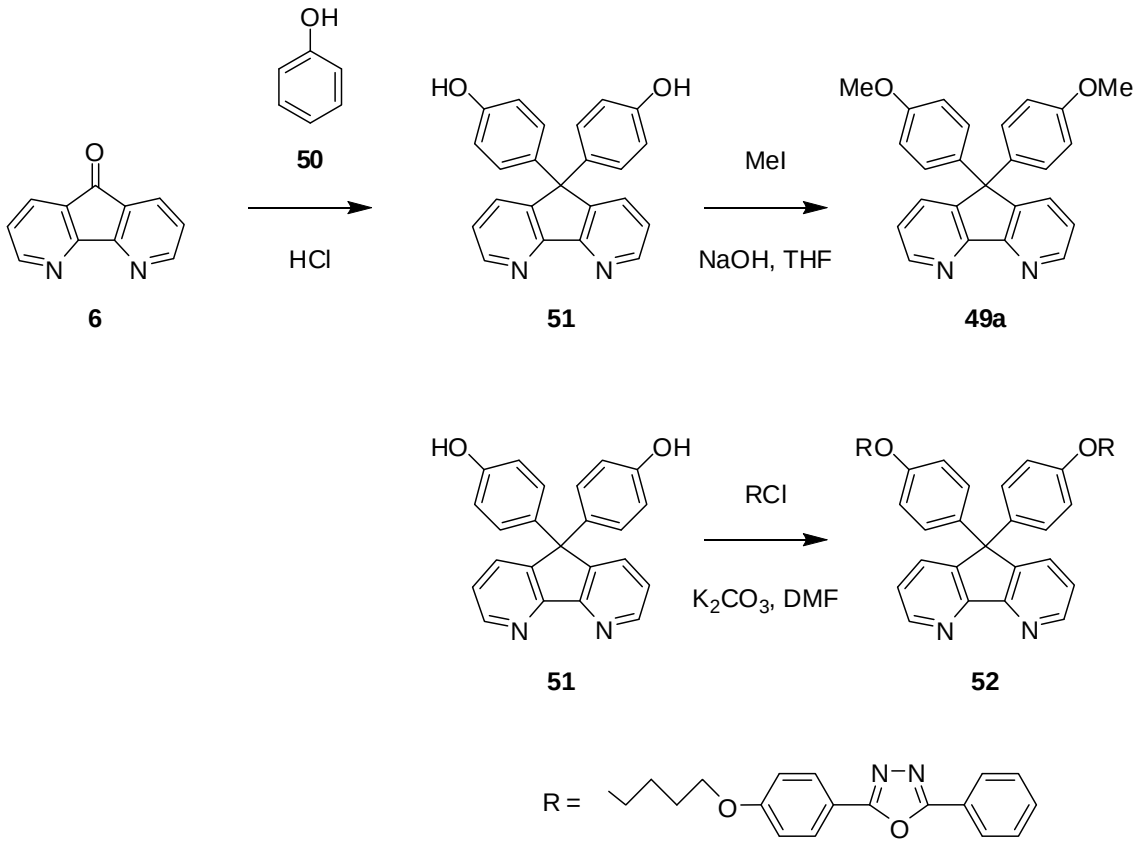

Scheme 13. Friedel-Crafts reactions of **6** in the presence of HCl.

(Figure 7a). The 4,5-diazafluorene ring system is planar. The methoxyphenyl groups are located above and below the plane. The bond lengths of the diazafluorene moiety are influenced by the introduction of bulky groups as compared to those of **1** (Figure 1). The molecular packing is characterized by a columnar structure along the *c* axis (Figure 7b). The methoxyphenyl groups overlap with each other in the column. The interplanar distance and the centroid-centroid distances between the benzene rings are 3.87(1) and 4.07(1) Å, respectively. The 4,5-diazafluorene units form a coil-like structure.

(a)

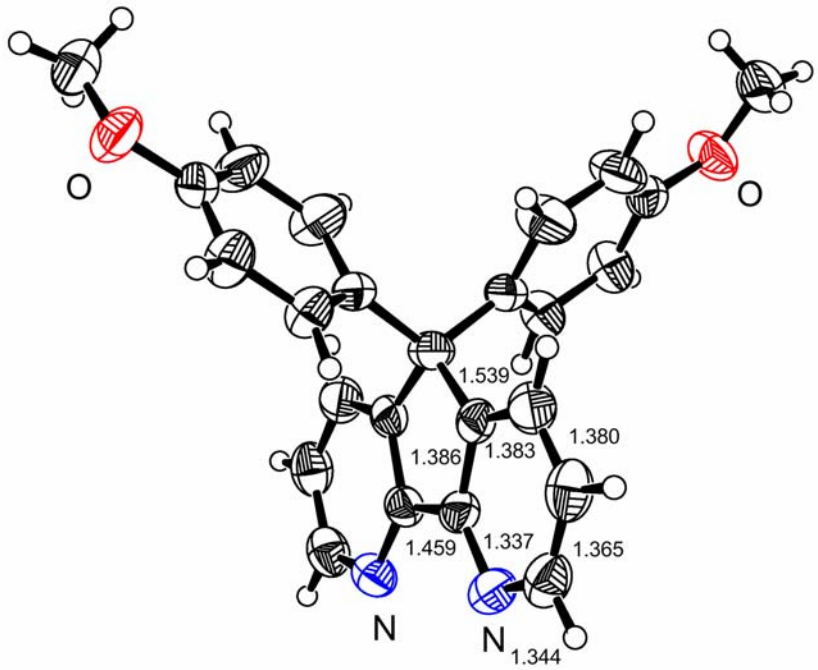

(b)

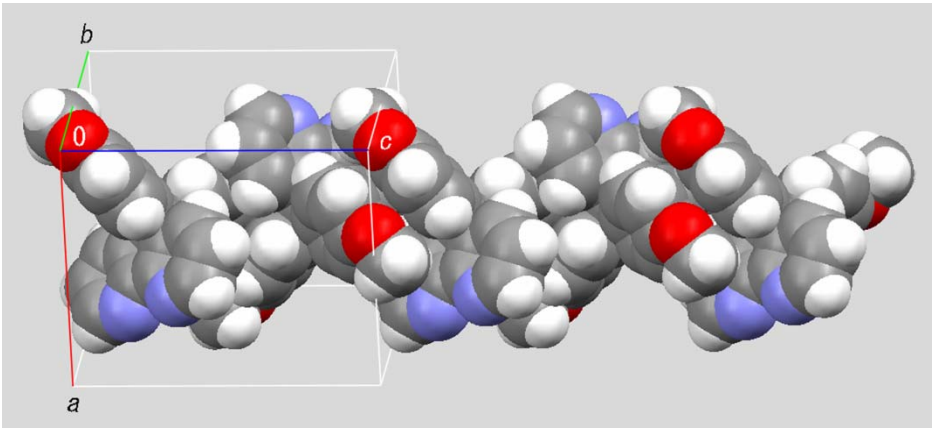

Figure 7. Crystal structure of **49a**: (a) molecular structure with bond lengths (Å); (b) molecular packing (*Acta Cryst.*, 2007, **E63**, o4612).

Wong *et al.*[20] reported an intramolecular Friedel-Crafts reaction (Scheme 14). Compound (**6**) reacted with arylmagnesium iodide (**53**) to afford compound (**54**) with a yield of 93%. The intramolecular

cyclization of **54** in which sulfuric acid was used as a catalyst provided 4,5-diaza-9,9′-spirobifluorene (**55**) with a yield of 75% in the form of a light brown solid. This compound was used as an electron-injecting unit for a highly efficient blue emitter in the study of EL devices.

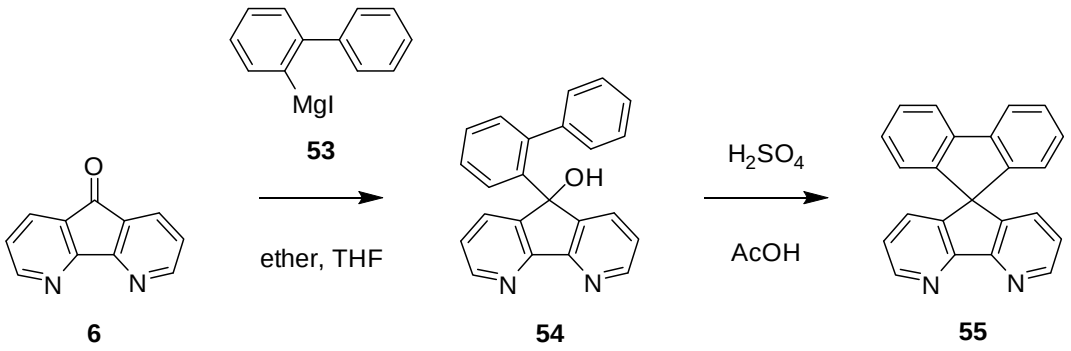

6 **54** **55**

Scheme 14. Intramolecular Friedel-Crafts reaction of **54**.

G. Direct arylation of 4,5-diazafluorene

The direct arylation and alkylation of the 2,2′-bipyridyl moieties are useful to produce unique building blocks in materials science. These reactions have been investigated for compounds such as 2,2′-bipyridyl (bpy), 1,10-phenanthroline (phen), and 2,2′:6′,2″-terpyridine (terpy). Direct arylation is able to introduce two phenyl groups into the compounds, and the yields of diphenyl (dp) products have been reported as 35% (dp-bpy), 70% (dp-phen), and 21% (dp-terpy).[21] We studied the direct arylation of compound (**49a**) in order to extend the π-electron system of 4,5-diazafluorene (Scheme 15).[22]

Compound (**49a**) reacted with 3.5 molar equiv. of phenyllithium (PhLi) in toluene, and this was followed by an oxidation reaction with MnO_2 to afford compound (**57a**) and monosubstituted compound (**56a**) with yields of 3% and 42%, respectively. A reaction involving 10 molar equiv. of PhLi and compound (**49a**) resulted in a similar yield. Thereafter, compound (**57a**) was obtained with a yield of 55% by the direct arylation of **56a** using 1.2 molar equiv. of PhLi. For the purpose of preparing derivatives with high electron affinities, the introduction of trifluoromethyl-substituted phenyl groups was examined. Compounds (**56b**)–(**56d**) were obtained with yields of 43–63% and compounds (**57b**)–(**57c**) were prepared with yields of 32 and 39% by using 1.2 molar equiv. of the corresponding aryllithium reagents. However, compound (**57d**) was not obtained from compound (**56d**) owing to steric hindrance among the 3,5-bis(trifluoromethyl)phenyl groups. Compounds (**57**) were purified by sublimation to afford colorless crystals (**57a**: mp = 271–272 °C, **57b**: mp = 251–252 °C, **57c**: mp = 209–210 °C).

Figure 8 shows the molecular structure and molecular packing of **57a** obtained from X-ray crystallographic analysis (CCDC 603473).[22] The molecule has extended π-conjugation with dihedral

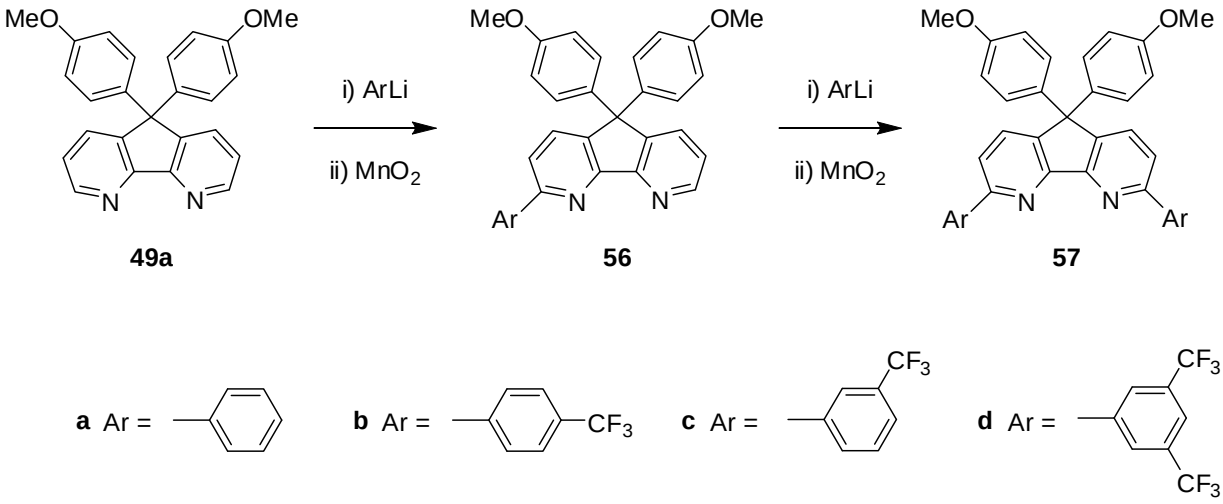

Scheme 15. Direct arylation of **49a** and **56**.

(a)

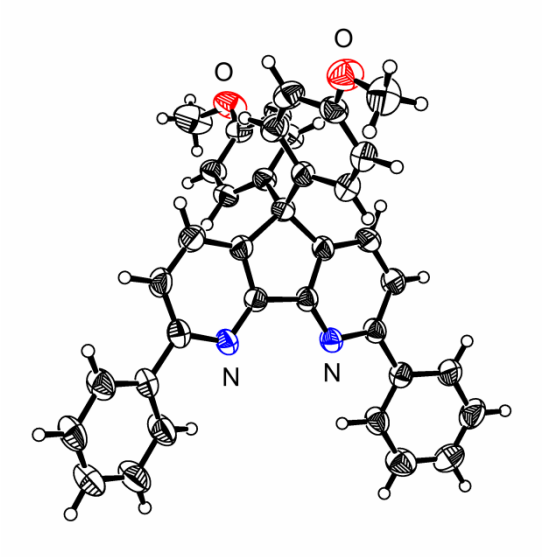

(b)

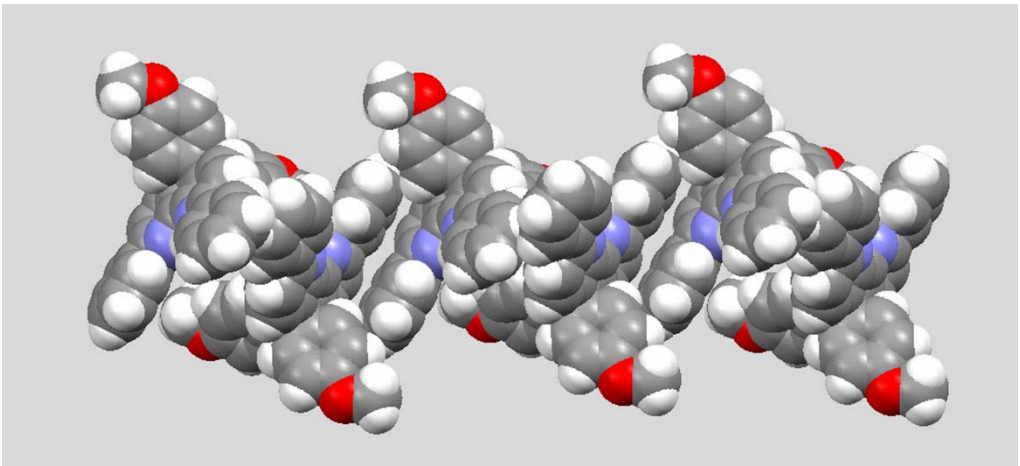

Figure 8. Crystal structure of **57a**: (a) molecular structure; (b) molecular packing (CCDC 603473).

angles of 13.5° and 15.9° between the diazafluorene moiety and the phenyl groups. The molecules are stacked along the *a* axis, and the diazafluorene moieties were observed to overlap in the column. The interplanar distance and the centroid-centroid distance between the pyridine and benzene rings are 4.41 and 4.49 Å, respectively. The extension of the π-electron system of **49a** leads to a modification of the packing mode in the column as compared to that shown in Figure 7b.

4. PROPERTIES AND APPLICATIONS OF 4,5-DIAZAFLUORENES

In this section, functional materials containing 4,5-diazafluorenes and their properties are described. These materials are investigated as electron-transporting materials and organic emitters in EL devices, emissive metal complexes, sensing elements, solar sensitizers, and DNA photocleaving agents.

A. Electron affinity and electron-transporting properties

Studies on carrier-transporting materials in organic EL devices have been of great interest since the effective recombination balance between electrons and holes in the emitting layers affords high EL efficiency and a long EL lifetime.[23] A variety of materials with high electron affinities have been synthesized and investigated for their role as electron-transporting layers.[24] Recently, electron-transporting materials have been also used in hole-blocking layers in EL devices comprising phosphorescent materials such as iridium and platinum complexes to obtain high quantum efficiencies. 2,9-Dimethyl-4,7-diphenyl-1,10-phenanthroline (BCP) is one of the most powerful electron-transporting and hole-blocking materials that provided external quantum efficiencies of 8.0 and 13.7% in combination with *fac*-tris(2-phenylpyridine)iridium [$Ir(ppy)_3$] in a 4,4′-bis(carbazol-9-yl)-1,1′-biphenyl (CBP) host.[25] With regard to this, we synthesized 9,9′-diaryl-4,5-diazafluorene (**49a**)–(**49c**) as a new type of material (Scheme 12) and investigated the application of **49a** in EL devices (Figure 9).[17]

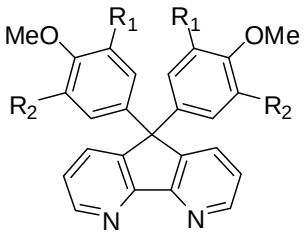

49a $R_1 = R_2 = H$

49b $R_1 = OMe$, $R_2 = H$

49c $R_1 = OMe$, $R_2 = OMe$

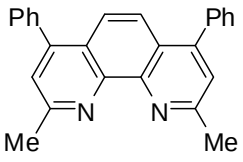

BCP

Figure 9. Structure of compounds (**49**) and BCP.

The absorption maxima of **49** were observed around 323 and 316 nm in dichloromethane (Table 1) and they were observed to be shifted to a longer wavelength as compared to those of BCP. The HOMO–LUMO energies of **49** were found to be 3.5–3.6 eV according to the absorption edges. These values are comparable to that of BCP. The cyclic voltammetry (CV) of **49** in DMF showed reversible one-electron redox waves. The half-wave reduction potentials are listed in Table 1. Although the reduction potentials are slightly lower than that of BCP, it was found that the energy levels of LUMOs are very close to that of BCP.

Table 1. Absorption maxima and edges and half-wave reduction potentials

Compound	λ_{max} (log ε)/nm[a]	λ_{edge}/eV[a]	$E_{1/2}^{red}$/V[b]
49a	324 (4.05), 316 (4.01)	3.6	−2.48
49b	323 (3.96), 316 (3.97)	3.5	−2.48
49c	323 (3.99), 316 (3.98)	3.6	−2.54
BCP	312sh (4.10), 280 (4.63)	3.5	−2.39[c]

[a]In CH_2Cl_2. [b]0.1 M *n*-Bu_4NClO_4 in DMF, Pt electrode, scan rate 500 mV s^{-1}, V vs. Fc/Fc^+.
[c]E_{pc} +0.03 V.

In order to investigate the electron-transporting and hole-blocking ability of the diazafluorene derivatives, EL devices using **49a** were fabricated, as shown in Figure 10a. *N*,*N*′-Diphenyl-*N*,*N*′-bis(3-methylphenyl)-1,1′-biphenyl-4,4′-diamine (TPD), $Ir(ppy)_3$, and CBP were used for the hole-transporting layer, emitter, and carrier combination host, respectively. For the cathode, an Al electrode with a LiF buffer layer was employed. Four types of electron-transporting layers (ETLs) were examined (devices 1–4). The ETL of device 1 comprised only compound (**49a**). The ETLs of devices 2 and 3 were formed by using the combination of **49a** with tris(8-hydroxyquinoline)aluminum (Alq_3) and 2,5-bis(bipyridyl)-1,1′-dimethyl-3,4-diphenylsilole (PyPySPyPy), respectively. BCP was employed as a reference for the ETL of device 4. Figure 10b shows the current density–applied voltage characteristics of the EL devices. The current density of device 1 is lower than that of device 4 in the range of the applied voltage, indicating that the electron-transporting ability of **49a** is inferior to that of BCP. The current density of the EL device is slightly improved in devices 2 and 3. All the devices began to emit at applied voltage of 3 V. The emission spectra from devices 1–3 were coincident with that from device 4, implying the display of phosphorescence by the $Ir(ppy)_3$ emitters in the devices. Figure 10c shows the effect of the external EL efficiency on the current density. The efficiency of device 1 is higher than that of device 4 within the measured current density, indicating a more effective recombination at the emitting layer of device 1. Compound (**49a**) is superior to BCP as a hole-blocking

material. The EL efficiency of device 2 is identical to that of device 1. On the other hand, a significant increase in the efficiency was observed in device 3. Thus, the efficiency is 1.5 times higher than that of device 4. The maximum external quantum efficiency reached 18% in device 3, and this value is close to the theoretical limit of approximately 20% from simple classical optics.[26] In addition, the maximum power luminous efficiency of device 3 was above 45 Lm W^{-1}, although the device was driven at a relatively high voltage.

(a) ITO/TPD (50 nm)/4.8%-Ir(ppy)$_3$:CBP (20 nm)/ETL (30 nm)/LiF (1 nm)/Al (70 nm).
device 1 (○) : ETL = **49a** (30 nm)
device 2 (□) : ETL = **49a** (10 nm) + Alq_3 (20 nm)
device 3 (△) : ETL = **49a** (10 nm) + PyPySPyPy (20 nm)
device 4 (×) : ETL = BCP (30 nm)

(b)

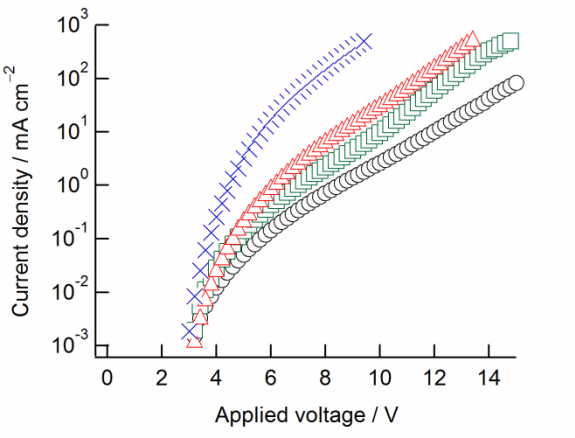

(c)

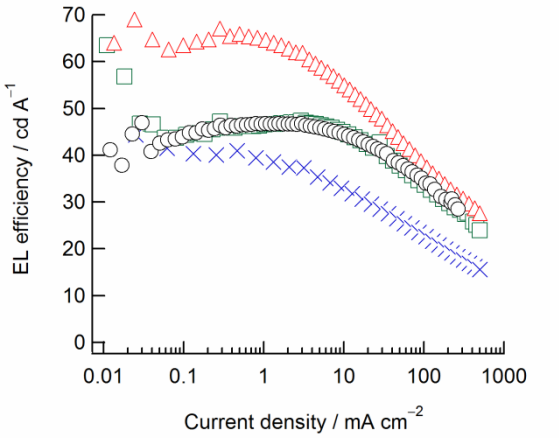

Figure 10. EL devices fabricated by Ir(ppy)$_3$ and **49a**: a) EL structures, b) current density–applied voltage curves, c) EL efficiency–current density curves.

B. Improvement of electron-transporting properties

As described above, the phosphorescent EL devices using compound (**49a**) demonstrated high EL efficiency because of the significant hole-blocking ability of the compound. However, the electron-transporting ability of **49a** was not as high as that of BCP. The EL device using both compound (**49a**) and PyPySPyPy exhibited a high external quantum efficiency of 18% due to the improved electron injection into the phosphor. This efficiency is close to the theoretical value. In order to improve the electron-transporting ability of compound (**49a**), we studied the extension of the π-electron system by direct arylation to afford compounds (**57a**)–(**57c**) (Figure 11).[22]

The UV spectra of compounds (**57a**)–(**57c**) in dichloromethane exhibited absorption bands in the same wavelength region due to the extended π-conjugation. The maxima are summarized in Table 2. These

maxima are red-shifted as compared to the maximum of **49a**. The HOMO–LUMO energy gaps of compounds (**57a**)–(**57c**) were found to be 3.3 eV from the absorption edges. This value is smaller than that of **49a**. The CV of compounds (**57**) revealed the presence of reversible reduction waves. The half-wave reduction potentials indicate that the introduction of trifluoromethylphenyl groups increases the electron affinities of the diazafluorene moieties.

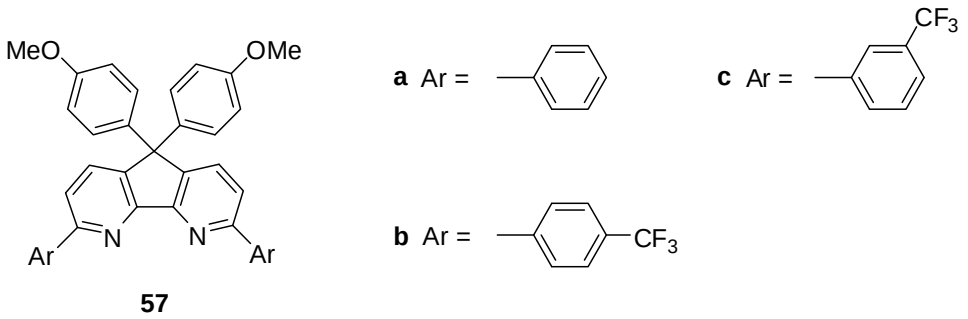

57

Figure 11. Structure of 3,6-diaryl-4,5-diazafluorenes (**57**).

Table 2. Absorption maxima and edges and half-wave reduction potentials

Compound	λ_{max} (log ε)/nm[a]	λ_{edge}/eV[a]	$E_{1/2}^{red}$/V[b]
57a	348 (4.32)	3.3	−2.45
57b	347 (4.34)	3.3	−2.32
57c	346 (4.31)	3.3	−2.34
49a	324 (4.05)	3.6	−2.48

[a]In CH_2Cl_2. [b]0.1 M *n*-Bu_4NClO_4 in DMF, Pt electrode, scanning rate 500 mV s^{-1}, V vs. Fc/Fc^+.

In order to investigate the electron-transporting properties of compounds (**57**), a phosphorescent EL device using compound (**57b**) was fabricated: ITO/TPD (50 nm)/Ir $(ppy)_3$: CBP (20 nm)/**57b** (30 nm)/LiF (1 nm)/Al (70 nm) (device 5). In addition, another EL device referred to as device 6 was examined by using BCP as the electron-transporting layer (ETL). Figure 12 shows a plot of the external quantum efficiency versus the current density. The efficiency of device 5 is higher than that of device 6. This result is attributed to the higher hole-blocking ability of compound (**57b**) as compared to that of BCP. The hole-blocking ability of **57b** resulted in the effective recombination of carriers in the emitting layer. The EL performance of device 5 (1000 cd m^{-2} at 9.4 V) was improved as compared to that of device 6 using compound (**49a**) (1000 cd m^{-2} at 13.4 V), indicating an increase in the electron injection to the

$Ir(ppy)_3$ emitter. This result is due to the higher electron-transporting ability of compound (**57b**) as well as the increase in the electron affinity resulting from the π-extension of the diazafluorene moiety.

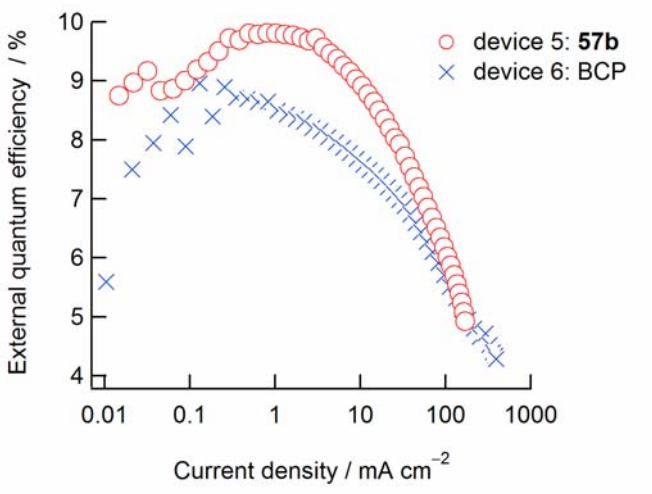

Figure 12. EL efficiency–current density curves; device 5 with **57b** (○), device 6 with BCP (×).

C. Electron-injection properties of EL emitters

Wong *et al.*[20] introduced 4,5-diazafluorene into ter(9,9-ditolylfluorene) (**58**) as an electron-injection unit to provide an efficient blue EL emitter (**59a**) (Figure 13). Compound (**58**) is one of the most efficient emitters for blue organic light-emitting diodes (OLEDs).[27] However, the electron affinity of **58** is relatively small, causing difficulties in electron injection from common cathode electrodes and imposing the requirement of an additional electron-transport layer with a more suitable electron-injection capability. Therefore, 4,5-diazafluorene has been facilely introduced as a functional substituent spirally linked to the conjugated terfluorene main chain. The resulting functionalized terfluorene (**59a**) possesses a more balanced electron-injection capability as compared to the parent compound (**58**). The device structure used was ITO/PEDT:PSS (30 nm)/TCTA (50 nm)/terfluorene (**58**) or (**59a**) (50 nm)/LiF (0.5 nm)/Al, where the conducting polymer polyethylene dioxythiophene:polystyrene sulfonate (PEDT:PSS) was used as the hole injection layer; 4,4′,4″-tri(*N*-carbazolyl)triphenylamine (TCTA), the hole-transport layer; terfluorenes, the emitting/electron-transport layer; and LiF, the electron-injection layer. Both devices exhibited pure blue EL. The quantum efficiencies of devices using **58** and **59a** were observed to be 0.4% and 1.6%, respectively. Furthermore, the device using **59a** exhibited a lower device voltage than the device using **58**. The EL properties of the blue emitter based on a terfluorene backbone were improved by the introduction of the 4,5-diazafluorene unit. In addition, a terfluorene analogue (**59b**) was synthesized and its bipolar properties were studied.[28]

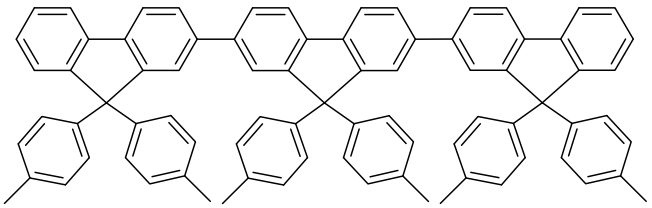

58

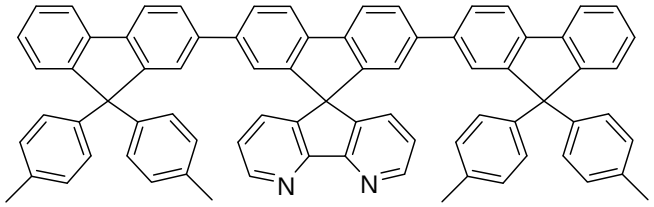

59a

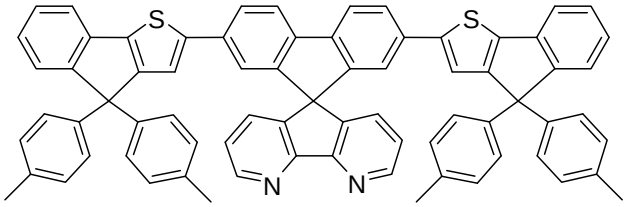

59b

Figure 13. Structure of organic emitters (**58**)–(**59**).

D. PET chromophore

Wong *et al.*[29] also synthesized a series of novel spiro-bridged bipolar chromophores by incorporating 4,5-diazafluorene units as electron acceptors and aryl amino groups as electron donors (**60**)–(**61**) (Figure 14). The perpendicular arrangement of the donor (D) and acceptor (A) limits the degree of D–A interaction in the ground state and allows an efficient photoinduced electron transfer (PET) to occur in the excited state. The efficiency of this PET process was varied by altering the D–A distance and the electronic characteristics of the donor moiety. The PET behavior of the bipolar molecule (**60a**) varied between the molecule's complexed and uncomplexed states, suggesting the potential for sensing metal ions. In particular, the complexation of **60a** with Sr^{2+} ions led to a significant change in the emission wavelength.

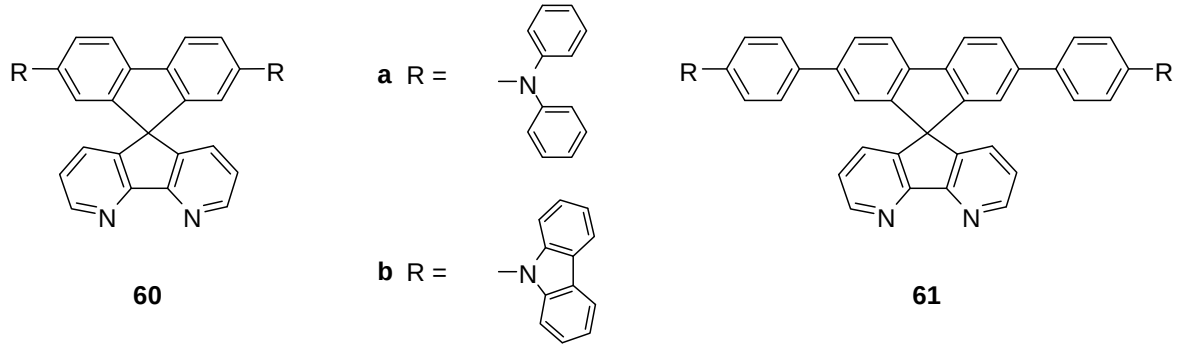

60 **61**

Figure 14. Structure of PET chromophores (**60**)–(**61**).

E. Ligand of emissive metal complexes

Among the red emission materials used in EL devices, europium(III) complexes have drawn tremendous attention because pure red emission can be produced by the electronic transition of the europium central ion. Furthermore, an internal quantum efficiency of 100% is theoretically possible because both singlet and triplet excitations can transfer their energy to the europium(III) ions. However, OLEDs containing these europium(III) complexes exhibited low EL efficiencies due to their poor carrier-transporting abilities. In this context, complexes (**62a**) and (**62b**) were prepared by Li *et al.* (Figure 15).[18] In complex (**62b**), an oxadiazole unit was introduced to the 4,5-diazafluorene ligand in order to improve the electron-transporting properties. For double-layer devices with a configuration of ITO/TPD (40 nm)/**62a** or **62b** (80 nm)/Mg:Ag (10:1) (200 nm), the brightness and EL efficiency of the device using **62b** was significantly improved as compared to those of the device using **62a** due to the improvement of the electron-transporting ability. A maximum brightness of 154 cd m^{-2} was obtained at 17 V in the device using **62b**. The luminance is approximately four times brighter than the device using **62a**. In addition, Xu *et al.*[30a] reported the synthesis, molecular structure, and optical properties of Eu complex (**63**) (Figure 15). Huang *et al.*[30b] synthesized Eu complex (**64**) and investigated the optical properties of its thin film.

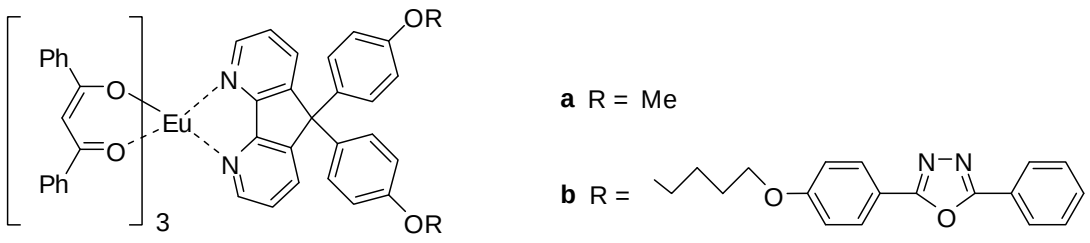

62

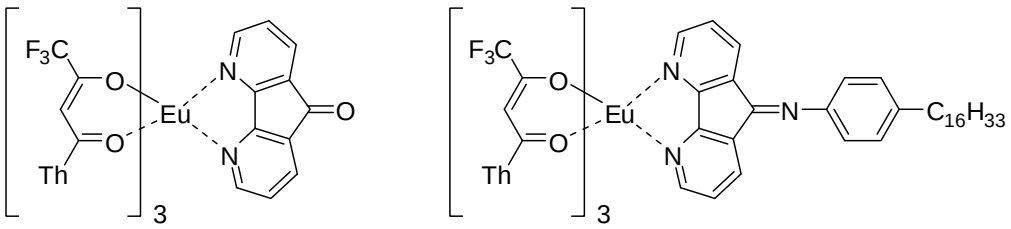

63 **64**

Figure 15. Structure of Eu complexes (**62**)–(**64**).

Cherry *et al.*[31] synthesized Ru(II) complexes (**65**)−(**67**) and investigated their optical properties (Figure 16). The emission maximum of **66** was observed at 609 nm under conditions at 77 K in EtOH/MeOH (4:1), and the maximum was red-shifted as compared to the maxima of $Ru(bpy)_3 \cdot 2PF_6$ (578 nm) and **65** (574 nm). Complex (**67**) showed very weak emission at the wavelength region around 585 nm. The emission quantum yield of **65** at 77 K was 0.56, and this value was higher than those of $Ru(bpy)_3 \cdot 2PF_6$ (0.33) and **66** (0.23). The emission lifetime was measured to be 5.2, 5.9, and 4.3 μs for $Ru(bpy)_3 \cdot 2PF_6$, **65**, and **66**, respectively.

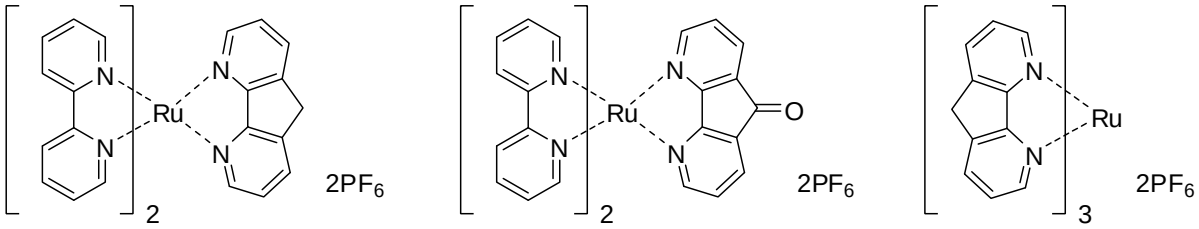

65 **66** **67**

Figure 16. Structure of Ru complexes (**65**)–(**67**).

Rillema *et al.*[32] synthesized a series of bimetallic Ru(II) complexes bridged by heterocyclic ligands (**68**)–(**70**) (Figure 17). These complexes showed metal-to-ligand charge-transfer (CT) absorptions and π–π* transitions in the 450 and 300 nm regions, respectively. These maxima were similar to those of complexes (**72**) and (**73**). The CV of **68** exhibited a reversible oxidation wave and four reversible reduction waves. Each of the two reductions at −0.29 and −0.52 V vs. saturated sodium calomel electrode (SSCE) was a one-electron process associated with ligand (**21**). The single oxidation at +1.38 V involved two one-electron processes associated with each of the ruthenium centers. Each of the remaining two waves located at −1.45 and −1.68 V involved two one-electron processes related to the reduction of the 2,2′-bipyridyl ligands at each reduction center. The CVs of **69** and **70** were similar to the CV of **68**. Thus, these complexes showed multiredox behavior. Complexes (**71**)–(**73**) exhibited an irreversible reduction wave at potentials between −0.86 and −0.94 V owing to the reduction of the ligand moieties, although the oxidation of the ruthenium centers and the reduction of bipyridyl ligands were observed to be similar to those of complex (**68**). Compounds (**68**)–(**73**) exhibited emission only in a glassy matrix at 77 K and at low temperatures in solution. The emission lifetimes at 77 K in EtOH/MeOH (4:1) glass were around 5 ± 1 μs.

68 $[(bpy)_2Ru(\mathbf{21})Ru(bpy)_2](PF_6)_4$ **69** $[(bpy)_2Ru(\mathbf{17})Ru(bpy)_2](PF_6)_4$

70 $[(bpy)_2Ru(\mathbf{18})Ru(bpy)_2](PF_6)_4$ **71** $[(bpy)_2Ru(\mathbf{19})Ru(bpy)_2](PF_6)_4$

72 $[(bpy)_2Ru(\mathbf{20})](PF_6)_2$ **73** $[(bpy)_2Ru(\mathbf{16})](PF_6)_2$

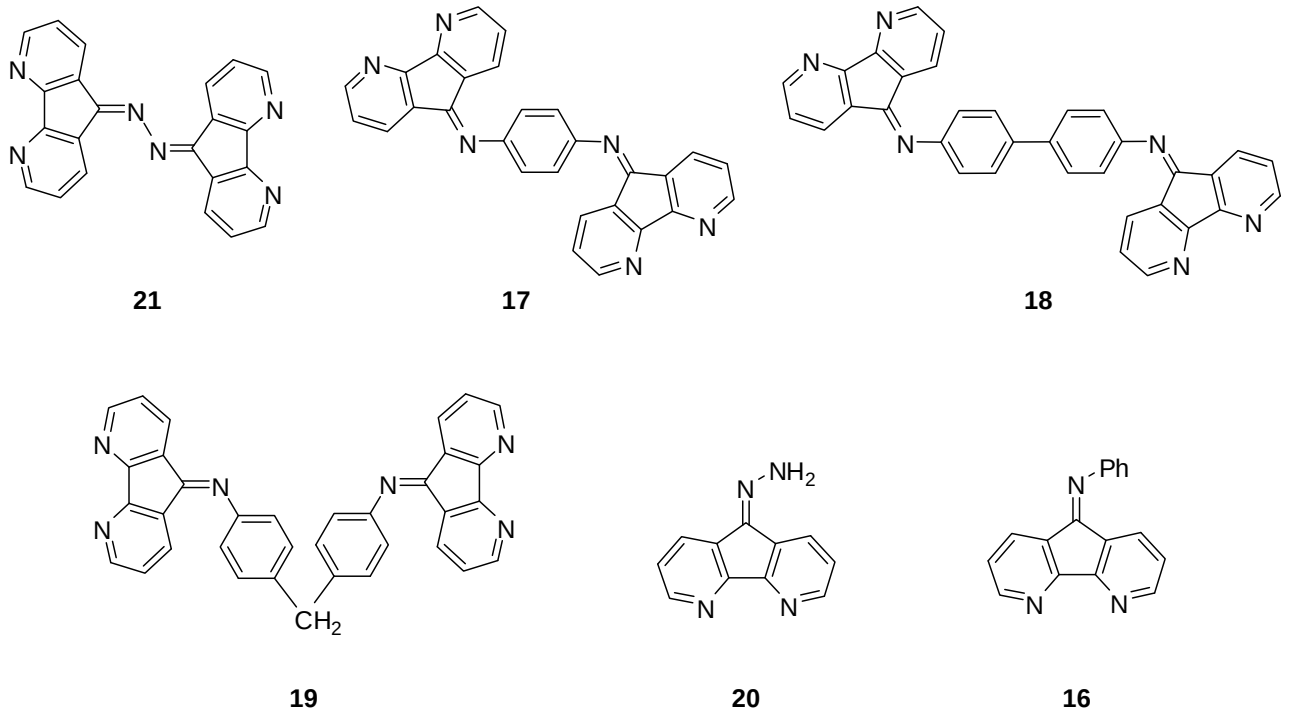

Figure 17. Structure of Ru complexes (**68**)–(**73**).

F. Dye sensitizer

The study of dye-sensitized solar cells has attracted considerable attention since the devices are expected to be fabricated at low cost and to show superior performance. Grätzel *et al.* reported high solar-energy-to-electricity conversion efficiencies (above 10%) using nanocrystalline TiO_2 technology.[33] Ruthenium(II) complexes with polypyridyl ligands such as 2,2′-bipyridyl, 2,2′:6′,2″-terpyridine, and 1,10-phenanthroline, which have been widely investigated, are effective CT sensitizers. In this context, we have prepared a red ruthenium complex (**74**) that contains 9,9-bis(4-methoxyphenyl)-4,5-diazafluorene (**49a**) as a polypyridyl ligand (Figure 18).[34] This ligand showed good performance as an electron-transporting material in organic EL devices due to its high electron affinity. The properties of complex (**74**) were investigated as a sensitizer of the Grätzel cell as compared to those of the *cis*-bis(thiocyanato-*N*)bis(4,4′-tetrabutylammonium hydrogen dicarboxylato-2,2′-bipyridine-κ^2N)ruthenium(II) dye (red dye N719).

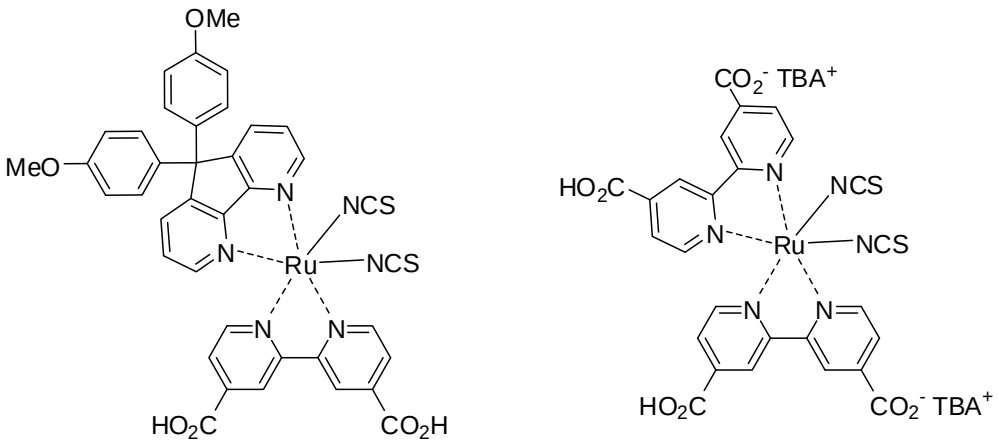

74 N719

Figure 18. Structure of dey sensitizers.

The UV–vis absorption spectrum of **74** in methanol is shown in Figure 19 and is observed to be similar to that of N719. The metal-to-ligand charge-transfer (MLCT) band of complex (**74**) extends to 700 nm, and the maximum was observed at 525 and 396 nm. These values are slightly red-shifted relative to those of N719 (521 and 380 nm).

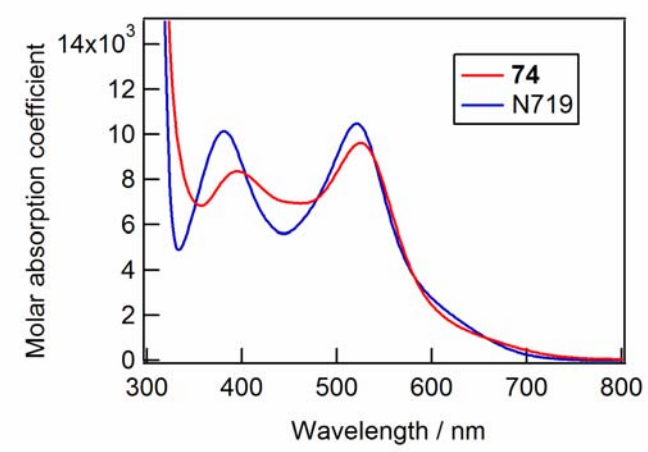

Figure 19. UV–vis absorption spectra of **74** and N719.

Nanocrystalline TiO_2 films were coated with dyes by dipping in solutions of complex (**74**) (cell 1) and N719 (cell 2) in acetonitrile-*tert*-butanol (1:1) for three days. Each dye-coated TiO_2 electrode was incorporated into a thin-layer sandwich-type cell with a Pt-sputtered transparent conducting oxide (TCO; F-doped SnO_2), a counter electrode, and an organic electrolyte solution. The electrolyte was a solution of 1,2-dimethyl-3-propylimidazolium iodide (DMPII, 0.6 M), lithium iodide (LiI, 0.1 M), iodine (I_2, 0.05 M), and 4-*tert*-butylpyridine (TBP, 0.5 M) in methoxyacetonitrile. The performance of the solar cell

was measured under irradiation with AM 1.5 solar light (100 mW cm^{-2}). Figure 20 shows the photocurrent–voltage curves for solar cells 1 and 2. The conversion efficiency (η) of cell 1 was recorded to be 7.3% for a short-circuit photocurrent density (J_{sc}) of 14.5 mA cm^{-2}, an open-circuit photovoltage (V_{oc}) of 0.68 V, and a fill factor of 0.74. On the other hand, an efficiency of η = 7.0% for J_{sc} = 13.7 mA cm^{-2}, V_{oc} = 0.70 V, and a fill factor of 0.73 was observed for cell 2. Thus, the conversion efficiency of cell 1 was slightly higher than that of cell 2; this result was due to an increase in the photocurrent density in cell 1 because the diazafluorene ligand inhibited the recombination of charge carriers to a greater extent.

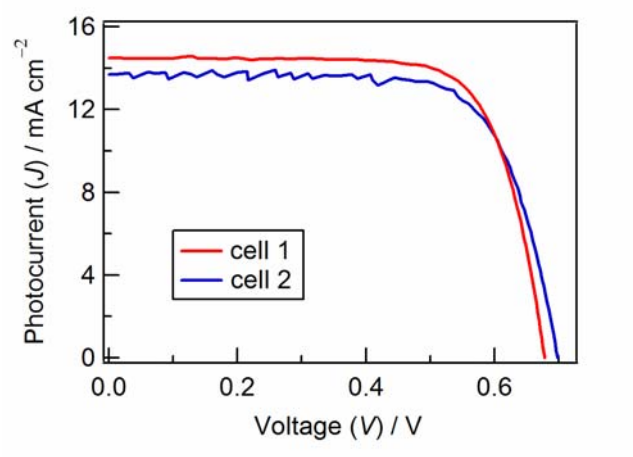

Figure 20. Photocurrent–voltage characteristics of cell 1 (**74**) and cell 2 (N719).

G. DNA photocleaving agent

Zaleski *et al.*[35] synthesized bis(9-diazo-4,5-diazafluorene)copper(II) nitrate (**75**) that is employed as an effective DNA photocleaving agent under anaerobic conditions using visible light. The complex represents a potential model for the action of kinamycin antitumor antibiotics such as kinamycin C (Figure 21).

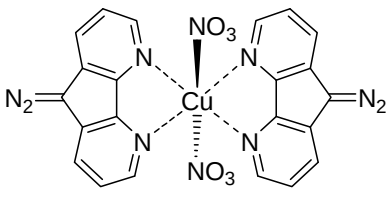

75

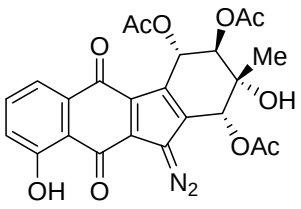

kinamycin C

Figure 21. DNA photocleaving agent (**75**).

In conclusion, we have discussed the chemistry and applications of 4,5-diazafluorene derivatives, which have unique molecular structures, reactivities, and properties different from those of 2,2′-bipyridyl and 1,10-phenanthroline. Furthermore, their applications as functional materials such as electron-transporting materials, organic emitters, emissive complexes, sensing elements, solar sensitizers, and DNA photocleaving agents have been widely investigated. The study of 4,5-diazafluorene is expected to continue to attract considerable attention.

REFERENCES

1. M. J. Plater, S. Kemp, and E. Lattmann, *J. Chem. Soc., Perkin Trans. 1*, 2000, 971.
2. I. F. Eckhard and L. A. Summers, *Aust. J. Chem.*, 1973, **26**, 2727.
3. a) R. P. Thummel and F. Lefoulon, *J. Org. Chem.*, 1985, **50**, 666. b) Y. Jahng, J. Hazelrigg, D. Kimball, E. Riesgo, F. Wu, and R. P. Thummel, *Inorg. Chem.*, 1997, **36**, 5390.
4. a) G. Kempter and W. Stoss, *J. Prakt. Chem.*, 1963, **21**, 198. b) P. Belser and A. von Zelewsky, *Helv. Chim. Acta*, 1980, **63**, 1675.
5. M. Riklin, A. von Zelewsky, A. Bashall, M. McPartlin, A. Baysal, J. A. Connor, and J. D. Wallis, *Helv. Chim. Acta*, 1999, **82**, 1666.
6. H.-K. Fun, K. Sivakumar, D.-R. Zhu, and X.-Z. You, *Acta Cryst.*, 1995, **C51**, 2076.
7. K. Kloc, J. Młochowski, and Z. Szulc, *Heterocycles*, 1978, **9**, 849.
8. K. Sako, M. Kusakabe, and H. Tatemitsu, *Mol. Cryst. Liq. Cryst.*, 1996, **285**, 101.
9. a) Q.-Y. Zhu, Y. Zhang, J. Dai, G.-Q. Bian, D.-X. Jia, J.-S. Zhang, and L. Guo, *Chem. Lett.*, 2003, **32**, 762. b) Q.-Y. Zhu, J. Dai, D.-X. Jia, L.-H. Cao, and H.-H. Lin, *Polyhedron*, 2004, **23**, 2259. c) Q.-Y. Zhu, J. Dai, G.-Q. Bian, X. Wang, W. Yang, and Z.-M. Yan, *Synth. React. Inorg., Met.-Org. Chem.*, 2002, **32**, 1001.
10. Y. Wang and D. P. Rillema, *Tetrahedron*, 1997, **53**, 12377.
11. J. Młochowski and Z. Szulc, *Polish J. Chem.*, 1983, **57**, 33.
12. Z.-L. Lu, W. Xiao, Z.-N. Chen, X.-Y. Gong, S. S. S. Raj, I. A. Razak, and H.-K. Fun, *Acta Cryst.*, 2000, **C56**, 1017.
13. S. Bernhard and P. Belser, *Synthesis*, 1996, 192.
14. B. J. Kraft, H. J. Eppley, J. C. Huffman, and J. M. Zaleski, *J. Am. Chem. Soc.*, 2002, **124**, 272.
15. S. Bernhard and P. Belser, *Synth. Commun.*, 1996, **26**, 3559.
16. a) R. N. Warrener, A. B. B. Ferreira, and E. R. T. Tiekink, *Tetrahedron Lett.*, 1996, **37**, 2161. b) R. N. Warrener, A. B. B. Ferreira, A. C. Schultz, D. N. Butler, F. R. Keene, and L. S. Kelso, *Angew. Chem. Int. Ed. Engl.*, 1996, **35**, 2485.
17. K. Ono, T. Yanase, M. Ohkita, K. Saito, Y. Matsushita, S. Naka, H. Okada, and H. Onnagawa,

Chem. Lett., 2004, **33**, 276.

18. Z. Liu, F. Wen, and W. Li, *Thin Solid Films*, 2005, **478**, 265.
19. K. Ono, M. Tomura, and K. Saito, *Acta Cryst.*, 2007, **E63**, o4612.
20. K.-T. Wong, R.-T. Chen, F.-C. Fang, C. Wu, and Y.-T. Lin, *Org. Lett.*, 2005, **7**, 1979.
21. C. O. Dietrich-Buchecker, P. A. Marnot, and J. P. Sauvage, *Tetrahedron Lett.*, 1982, **23**, 5291.
22. K. Ono, K. Nagano, M. Suto, and K. Saito, *Heterocycles*, 2007, **71**, 799.
23. a) C. W. Tang and S. A. VanSlyke, *Appl. Phys. Lett.*, 1987, **51**, 913. b) C. Adachi, S. Tokito, T. Tsutsui, and S. Saito, *Jpn. J. Appl. Phys.*, 1988, **27**, L713.
24. G. Hughes and M. R. Bryce, *J. Mater. Chem.*, 2005, **15**, 94.
25. a) M. A. Baldo, S. Lamansky, P. E. Burrows, M. E. Thompson, and S. R. Forrest, *Appl. Phys. Lett.*, 1999, **75**, 4. b) T. Tsutsui, M.-J. Yang, M. Yahiro, K. Nakamura, T. Watanabe, T. Tsuji, Y. Fukuda, T. Wakimoto, and S. Miyaguchi, *Jpn. J. Appl. Phys.*, 1999, **38**, L1502.
26. G. Gu, D. Z. Garbuzov, P. E. Burrows, S. Venkatesh, S. R. Forrest, and M. E. Thompson, *Opt. Lett.*, 1997, **22**, 396.
27. K.-T. Wong, Y.-Y. Chien, R.-T. Chen, C.-F. Wang, Y.-T. Lin, H.-H. Chiang, P.-Y. Hsieh, C.-C. Wu, C. H. Chou, Y. O. Su, G.-H. Lee, and S.-M. Peng, *J. Am. Chem. Soc.*, 2002, **124**, 11576.
28. K.-T. Wong, T.-Y. Hwu, A. Balaiah, T.-C. Chao, F.-C. Fang, C.-T. Lee, and Y.-C. Peng, *Org. Lett.*, 2006, **8**, 1415.
29. K.-T. Wong, H.-F. Chen, and F.-C. Fang, *Org. Lett.*, 2006, **8**, 3501.
30. a) H.-B. Liu, B.-L. Li, H.-Q. Wang, and Z. Xu, *Chinese J. Chem.*, 2001, **19**, 766. b) K. Z. Wang, L. H. Gao, C. H. Huang, G. Q. Yao, X. S. Zhao, X. H. Xia, J. M. Xu, and T. K. Li, *Solid State Commun.*, 1996, **98**, 1075.
31. L. J. Henderson, Jr., F. R. Fronczek, and W. R. Cherry, *J. Am. Chem. Soc.*, 1984, **106**, 5876.
32. Y. Wang, W. J. Perez, G. Y. Zheng, D. P. Rillema, and C. L. Huber, *Inorg. Chem.*, 1998, **37**, 2227.
33. M. K. Nazeeruddin, F. De Angelis, S. Fantacci, A. Selloni, G. Viscardi, P. Liska, S. Ito, B. Takeru, and M. Grätzel, *J. Am. Chem. Soc.*, 2005, **127**, 16835.
34. K. Ono, H. Tanaka, M. Shiozawa, T. Motohiro, S. Kunikane, and K. Saito, *Chem. Lett.*, 2007, **36**, 892.
35. H. J. Eppley, S. M. Lato, A. D. Ellington, and J. M. Zaleski, *Chem. Commun.*, 1999, 2405.

Katsuhiko Ono was born in 1967 in Nagano. He received his Ph. D. degree from the Graduate University for Advanced Studies, Institute for Molecular Science, in 1995 under the supervision of Professor Yoshiro Yamashita. He was a JSPS fellow in 1994–1995 and a NEDO fellow in 1996–1999. He spent one year as a researcher at Dow Corning Asia Ltd. He moved to the Graduate School of Engineering, Nagoya Institute of Technology, as a research associate. His present research focuses on organic materials for OFETs, OLEDs, and solar cells.

Katsuhiro Saito is a Professor of the Nagoya Institute of Technology. He was born in Niigata in 1945. He obtained his Ph. D. degree from Tohoku University in 1974. He was appointed as a lecturer at the Nagoya Institute of Technology in 1974. He was promoted to associate professor in 1976 and to professor in 1996 at the Graduate School of Engineering, Nagoya Institute of Technology. His current research interests include organic chemistry, materials science, and supramolecular chemistry.